Science Translational Medicine
AAAS

# Supplementary Materials for

## Interleukin-6–dependent epithelial fluidization initiates fibrotic lung remodeling

Ian T. Stancil *et al.*

Corresponding author: David A. Schwartz, david.schwartz@cuanschutz.edu

*Sci. Transl. Med.* **14**, eabo5254 (2022)
DOI: 10.1126/scitranslmed.abo5254

**The PDF file includes:**



**Other Supplementary Material for this manuscript includes the following:**

## Materials and Methods

Mouse lung histology and immunofluorescence

At harvest, the left lung was inflated with 4% formalin at a pressure of 20 cm $H_2O$ for 5 min. The lung was then removed and placed in fresh 2% formalin overnight for fixation. Lungs were then embedded in paraffin, cut into 7 µm sections, and collected on positively charged glass slides. Alternatively, formalin-fixed lungs were placed into PBS containing 30% sucrose for 24 to 48 hours at 4ºC. The lungs were subsequently embedded in OCT compound (Fisher Scientific, 23-730-571) and sliced into 7 µm section using a cryostat.

For immunohistochemistry, tissues were heated in citrate buffer for antigen retrieval. Tissue was washed subsequently with PBS and permeabilized with Triton-X at 0.1% (Sigma-Aldrich, X100) in PBS and blocked in 5% bovine serum albumin for 1 hour at room temperature. Primary antibody was added to tissue and incubated overnight 4ºC. Subsequently, the slides were washed with PBS containing 0.1% Tween-20 at room temperature. The slides were stained with secondary antibodies for 1 hour at room temperature. Tissues were stained with DAPI at 1:20,000 (BioLegend, 422801) before being coverslipped.

Precision cut lung slice inhibitor treatments

The following inhibitors were utilized in the assessment of mouse airway epithelial function ex vivo: (S)-nitro-blebbistatin at 50 µM (Cayam Chemical, 13891), anti-mouse IL-6 and IL-6R at 50 µg/ml (BioXCell, BE0046 and BE0047, respectively), Ruxolitinib at 25 µM (Selleckchem, S1378), Saracatinib at 10 µM (Selleckchem, S1006). Briefly, inhibitors were added 2 hours prior to live cell imaging, and PCLS were continuously treated for the duration of imaging.

Hydroxyproline content determination

For bleomycin studies, the entire right lung was excised, submerged in 550 µl of PBS, and subsequently homogenized using Lysing Matrix D and FastPrep-24 bead beater (MP Biomedicals, Santa Ana, CA). Samples were then immediately frozen and stored at -80ºC. Thawed homogenates were hydrolyzed in a 1:1 volume of 12N hydrochloric acid at 100ºC overnight. Afterwards, 5 µl samples of hydrolyzed lung and hydroxyproline standards were plated in duplicate in 96-well plates and incubated for 20 min in 100 µl of 0.06 M chloramine T in citrate-acetate buffer, pH 6. Ehrlich's solution (100 µl; 1.2 M dimethylaminobenzaldehyde in 22% perchloric acid-n-propanol) was then added to each sample. After a 20-min incubation at 65 °C, plates were analyzed in a Synergy H1 plate reader (Biotek) at 550 nm for colorimetric analysis. Concentrations of each sample were determined by interpolation along a standard curve.

Bronchoalveolar lavage

Immediately following euthanasia, cannulated mouse tracheas were lavaged three times with 0.5 ml of PBS containing 0.6 mM EDTA. Cells were subsequently counted using a hemacytometer and spun onto slides using a Cytospin 4 (Thermo Fisher Scientific). The slides were stained with the Hema 3 kit (Thermo Fisher Scientific) and used for differential counts of total leukocytes, macrophages, lymphocytes, and neutrophils.

Immunofluorescence staining of in vitro cultures

Epithelial cells were fixed by the addition of 4% formalin in DPBS (Gibco, 14040133) to the apical and basal compartment of the transwell for ~30 minutes at room temperature. Transwells were washed subsequently with PBS and permeabilized with Triton-X at 0.1% (Sigma, X100) in PBS and blocked in 5% bovine serum albumin for 1 hour at room temperature. Primary antibody was added to the apical compartment of the transwell for >16 hours overnight on a rocker at 4ºC. Subsequently, cells were washed with PBS containing 0.1% Tween-20 at room temperature. Secondary antibodies, and/or Phalloidin-iFluor 647 at 1:2500 (Abcam, ab176759), were added to the apical compartment of the transwell for 1 hour at room temperature. Transwell membranes were then mounted onto glass slides with Fluoromount-G (SouthernBiotech, 0100-01) and visualized on an Olympus BX63 microscope (Olympus) or Keyence BZ-X810.

Epithelial-fibroblast co-culture

Primary human lung fibroblasts (HLFs) were obtained from control lungs not suitable for transplantation at National Jewish Health (IRB protocol HS-3209, approved by National Jewish Institutional Review Board under non-human subject research) in contract with the International Institute for the Advancement of Medicine and Donor Alliance. HLFs from patients with IPF were obtained from lung transplants at the University of Colorado Hospital (IRB protocol: 11-1664 or 18-0572, approved by the Colorado Multiple Institutional Review Board). Before donation, informed consent for research use was provided by families and/or donors directly. Briefly, pieces of lung tissue were placed into a tissue-culture dish and weighed down by a coverslip. Cells were cultured in DMEM supplemented with L-glutamine (Corning, 25-005-CI), penicillin/streptomycin, and 10% fetal bovine serum. These fibroblasts were then sub-cultured in t-75 flasks. All HLFs used in this study ($N = 4$) were seeded at passage 3.

Experimentally, HLFs were seeded into the bottom of wells of a 24-well plate at a density of 2,750 cells/cm$^2$ in DMEM supplemented with L-glutamine, penicillin-streptomycin, and 10% FBS. HLFs were cultured for 72 hours before initiation of co-culture with primary airway epithelial cells. Before starting co-culture the HLF media was changed to the standard primary airway cell culture media to prevent growth of airway cells in serum-containing media. Primary airway epithelial cells were seeded into 24-well transwells as per the described protocol (*20*), and the transwell was added to the plate containing HLFs. Co-culture was maintained through establishment of ALI until day 14 ALI.

For experiments involving inhibition of IL-6-related signaling, an identical co-culture protocol was followed until day 4 of ALI at which point the following inhibitors were added to the basal compartment of the co-culture: IL-6 neutralizing antibody at 10 ng/ml (R&D Systems, MAB206), IL-6R neutralizing antibody at 1 μg/ml (R&D Systems, MAB227), and recombinant human gp130 Fc chimera at 1 μg/ml (R&D Systems, 671-GP). The co-cultures were continuously cultured in the presence of these inhibitors until day 14 of ALI.

Quantitative RT-PCR

Cell lysis was completed by the addition of RLT and 2-mercaptoethanol to the apical compartment of the transwell and subsequent total RNA extraction was completed using the

RNeasy Mini Kit (Qiagen, 74104) and subsequently quantified using a NanoDrop spectrophotometer. Total RNA was reverse transcribed using the High-Capacity cDNA Reverse Transcription Kit (Applied Biosystems, 4368814). Gene expression was quantified by using TaqMan Advanced Master Mix (Invitrogen, 43-700-48) and TaqMan assays which were run in triplicate on the ViiA 7 Real-Time quantitative PCR machine. Unless otherwise specified, untreated epithelial cultures were used as baseline comparisons with beta-actin being used as the housekeeping gene. The delta-Ct method was utilized to determine cycle differences in gene expression across conditions. Primer and probe IDs are located in Table S4.

Immunoblotting

Epithelial cells were lysed in 2x Laemmli Sample Buffer (Bio-Rad, 1610737) supplemented with 5% 2-mercaptoethanol and 2x Halt Phosphatase Inhibitor Cocktail (Thermo Fisher Scientific, 78426). Briefly, sample buffer was added to the apical compartment of the transwell and proteins were isolated via mechanical disruption. Each loaded lane consisted of equal protein from $N = 4$ replicate wells from $n = 3$ independent donors. A 10% polyacrylamide gel (Bio-Rad, 4568036) was utilized for protein separation with subsequent transfer to a polyvinylidene difluoride membrane (Millipore Sigma, IPVH00010). Membranes were subsequently dried at room temperature for > 2 hours, rehydrated and blocked in Intercept Blocking Buffer (Li-COR, 927-60001) for 1 hour. Membranes were incubated >16 hours at 4ºC with primary antibody and subsequently washed and incubated with secondary antibodies for 1 hour at room temperature. Band visualization was completed using the Li-COR Odysessy CLx system with band quantification being performed in Image Studio. Briefly, to quantify phospho-proteins, each membrane was compared to an internal loading control (β-actin); once normalized, phospho-protein was quantified relative to total protein expression, which was also normalized to its own independent loading control.

Epithelial barrier function measurement

Epithelial barrier function was quantified by via transepithelial electrical resistance (TEER) utilizing a Millicell ERS-2 Voltohmeter (Millipore Sigma, MERS00002). Transwells were incubated with DPBS in the apical compartment for 15 minutes at 37ºC. The TEER probe was then inserted into the apical and basal compartment of the transwell and the resultant resistance reading in Ohms was recorded. Epithelial TEER was calculated by subtracting an empty transwell resistance (100 Ohms) from the recorded value and then multiplying by the surface area of a single 24-transwell (0.33 $cm^2$). TEER was recorded before any ligand and/or inhibitor treatment and then recorded after treatment to assess if there was any change in barrier function from the untreated condition, which was then compared back to an untreated well. TEER reported was the average of $N \geq 2$ wells from $n \geq 4$ donors.

Secreted protein detection

Secreted IL-6 family cytokines were detected by human Quantikine ELISA kits from R&D Systems. IL-6 (D6050), IL-6R (DR600), LIF (DLF00B), and IL-11 (D1100) were quantified following the manufacturer guidelines. Media from proximal ($n = 4$), distal ($n = 4$), and honeycomb ($n = 4$) cultures were collected at various days after the establishment of ALI. Cytokine concentration was determined via standard curve interpolation from a four parametric logistic curve fit.

Immunofluorescence quantification

For mean fluorescence quantification of cell-type markers in vitro, all images were acquired using identical settings and processed in the same manner. Images were acquired of a 10x field of view using a Keyence BZ-X810 microscope. Fluorescent images were separated by channel, and the mean gray value was measured using ImageJ. Care was taken to identify non-overlapping fields of view near the center of each Transwell membrane. Images were obtained from ≥3 donors with ≥3 fields of view per well and ≥2 independent wells.

For quantification of total $Krt5^+$ area in bleomycin-injured mouse lungs, 10x tile-scans were acquired of individual 7 μm thick lung slices using a Keyence BZ-X810 microscope. Images were stitched using accompanying Keyence software. Standardized threshold settings were used to measure the total area of $Krt5^+$ staining and $DAPI^+$ staining. $Krt5^+$ area was divided by $DAPI^+$ area to generate the percentage of $Krt5^+$ cysts per lung. Images were obtained from ≥5 sections from ≥5 mice per treatment condition. Sections were separated by ~150 μm to ensure representation from the entire lung. Average values were obtained for each mouse.

Cell shape analysis

Epithelial cell shape was determined in vitro or ex vivo via border delineation by F-actin or E-cadherin immunofluorescence, respectively. Images were subsequently processed in ImageJ removing background utilizing a rolling ball radius of 100 pixels. Background-subtracted images were then segmented in SeedWater segmenter (*60*). Utilizing established workflows (*20*, *30*), we quantified individual cell shape on the basis of aspect ratio and shape index for all cells within a given field of view. For each in vitro experimental condition at least 3 representative images were acquired from a minimum of 2 independent wells from $N = 4$ donors. Images were acquired at 40x and quantification is from ~ 1500 cells/condition. Ex vivo, epithelial quantification consisted of $n = 3$ mice (uninjured or H1N1) with 2 airways from each mouse being quantified in regions of detectable injury (as indicated by the occurrence of $Krt5^+$ cells). Color coded aspect ratios were achieved through adaptation of the ImageJ ROI Color Coder.

RNA-sequencing and analysis

As described above, total RNA was extracted using an RNeasy Mini Kit. RNA quality for RNA-sequencing was determined utilizing the Agilent 2200 TapeStation. mRNA libraries were prepared from 500 ng total RNA with TruSeq stranded mRNA library preparation kits (Illumina) and sequenced at an average depth of 92.4M reads on an Illumina NovaSeq 6000. Paired-end reads were aligned to the human genome using STAR and quality control was performed using RNA-SeQC. No samples were removed based on pre-defined QC metrics (<30 mean quality score, <85% mapped reads, >10% mitochondrial reads, and >50% PCR duplicates). Differential expression was assessed using DESeq2 (6*1*). Benjamini-Hochberg false discovery rate (FDR)-adjusted *p*-values <0.05 were considered significant. Pathway enrichment analyses were performed utilizing Enrichr (*62*,*63*).

Antibodies

For immunofluorescence in human tissue, we used the following antibodies: mouse anti-Ki67 at 1:500 (Cell Signaling Technology, 9449), chicken anti-KRT5 at 1:500 (BioLegend, 905901), rabbit anti-KRT17 (Abcam, ab109725), rabbit anti-YAP at 1:250 (Cell Signaling Technology, 14074), rabbit anti-MUC5B at 1:500 (Santa Cruz Biotechnology, clone H-300), and

mouse anti-MUC5AC at 1:500 (Invitrogen, MA5-12178). All secondary antibodies were purchased from Thermo Fisher Scientific and used at a concentration of 1:500. For immunofluorescence in mouse tissue, we used the following antibodies: rabbit anti-E-Cadherin at 1:250 (Cell Signaling Technology, 3195) and chicken anti-Krt5 at 1:500 (BioLegend, 905901). All secondary antibodies were purchased from Thermo Fisher Scientific and used at a concentration of 1:500.

For Western blotting, we used the following antibodies at the specified concentration: rabbit anti-β-actin at 1:2000 (Cell Signaling Technology, 4970), rabbit anti-phospho-YAP S127 at 1:1000 (Cell Signaling Technology, 13008), rabbit anti-phospho-YAP S357 at 1:1000 (Abcam, ab62751), and rabbit anti-total YAP at 1:1000 (abcam, ab52771). Secondary antibodies were purchased from Li-COR and used at a concentration of 1:10,000.

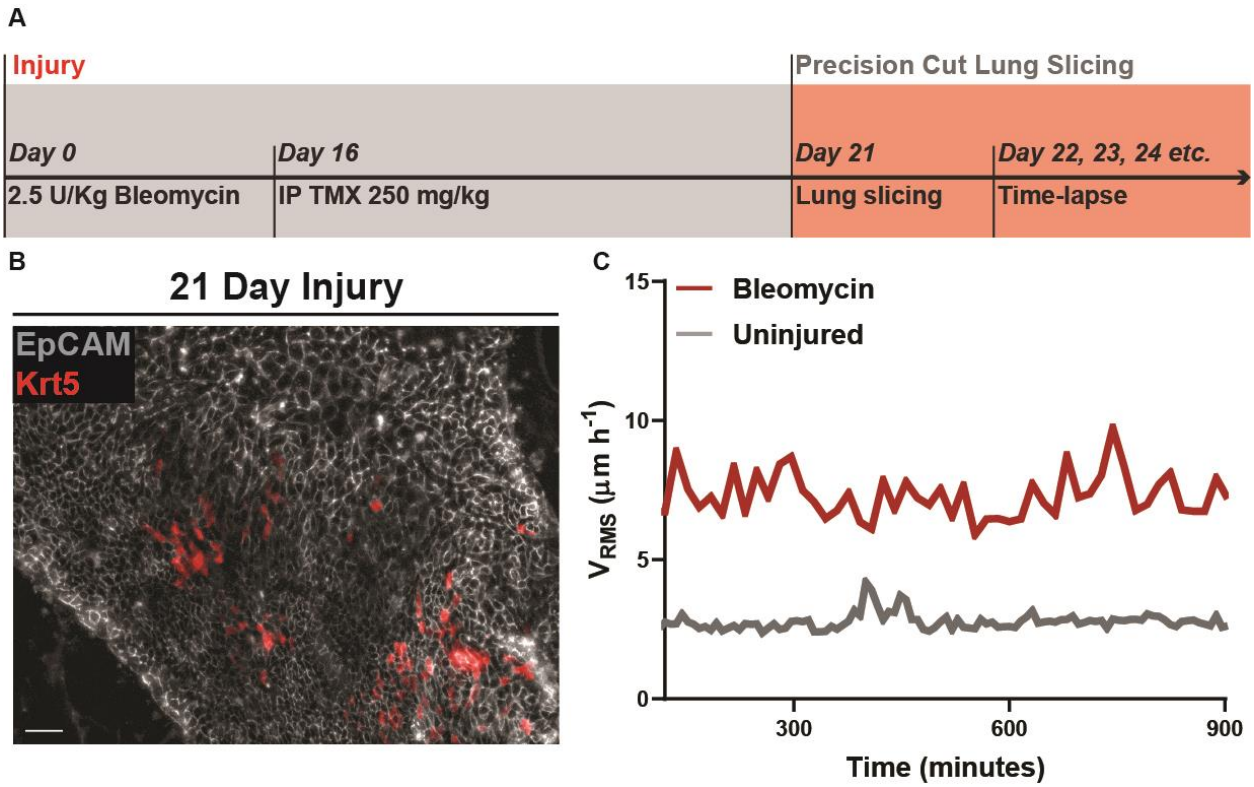


**Fig. S1. Bleomycin-induced lung injury includes airway epithelial fluidization.** (**A**) Timeline of bleomycin-induced lung injury and subsequent precision cut lung slicing. (**B**) Krt5$^{-}$TdTomato$^{+}$ cells present in the mouse airway 21 days after bleomycin injury. 100 μm scale bar shown. (**C**) Quantification of cellular dynamics as graphed by the mean of root mean-squared velocity ($V_{RMS}$) across all replicates. Mouse experiments were independently performed $N \geq 2$ times with $n \geq 4$ donors.

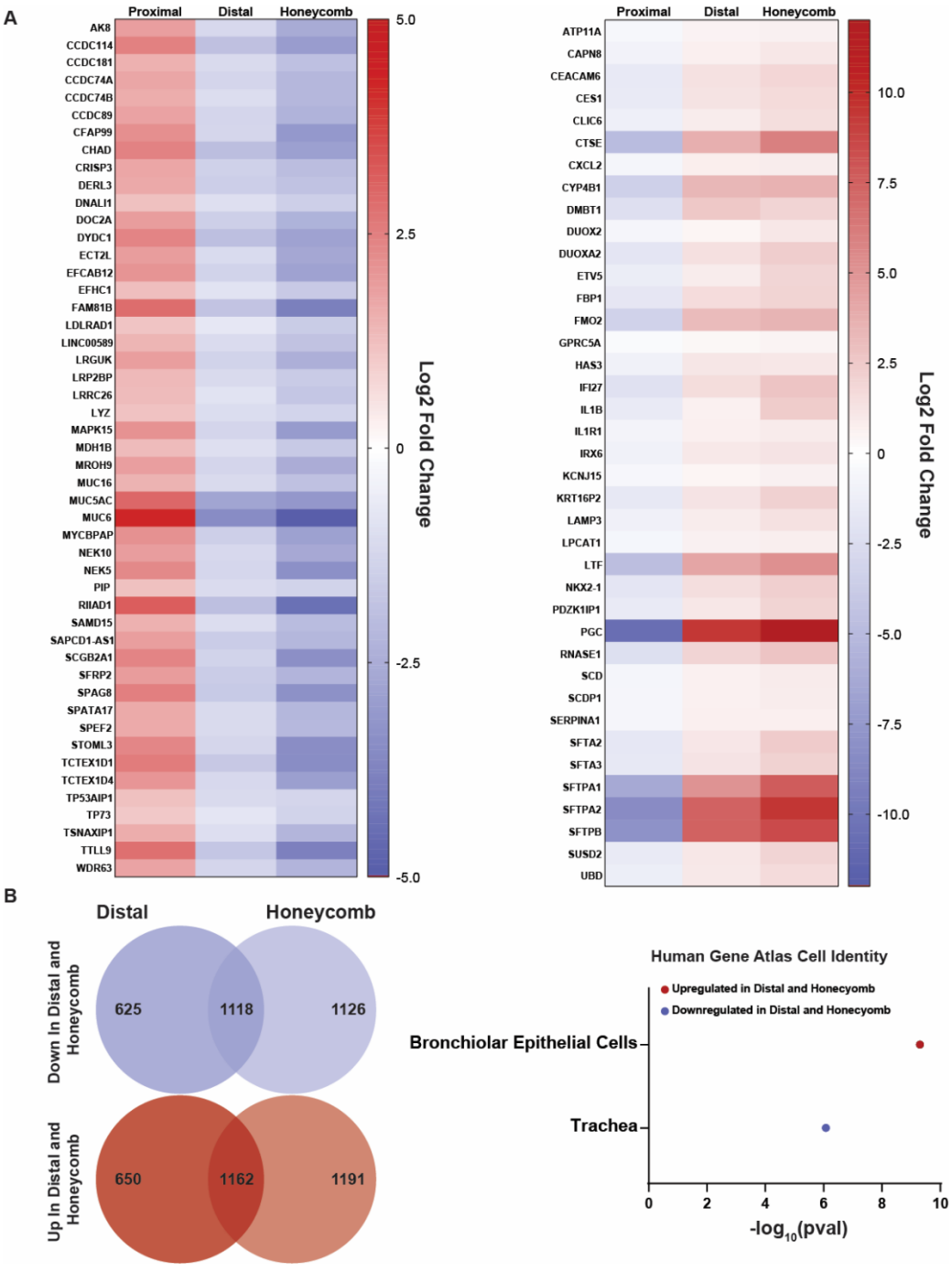


**Fig. S2. Regional cultures express appropriate cell-type markers.** (**A**) Representative genes from bulk RNA-sequencing of proximal, distal, and honeycomb air liquid-interface cultures at day 14. Left: proximal airway-associated genes are up-regulated in the proximal airway culture and down-regulated in the distal and honeycomb cultures. Right: distal airway-associated genes are down-regulated in the proximal airway culture and up-regulated in the distal and honeycomb cultures. (**B**) Left: differentially regulated genes in distal and honeycomb compared to proximal cultures. Right: human gene atlas cell identity for shared differentially regulated genes in distal and honeycomb compared to proximal cultures.

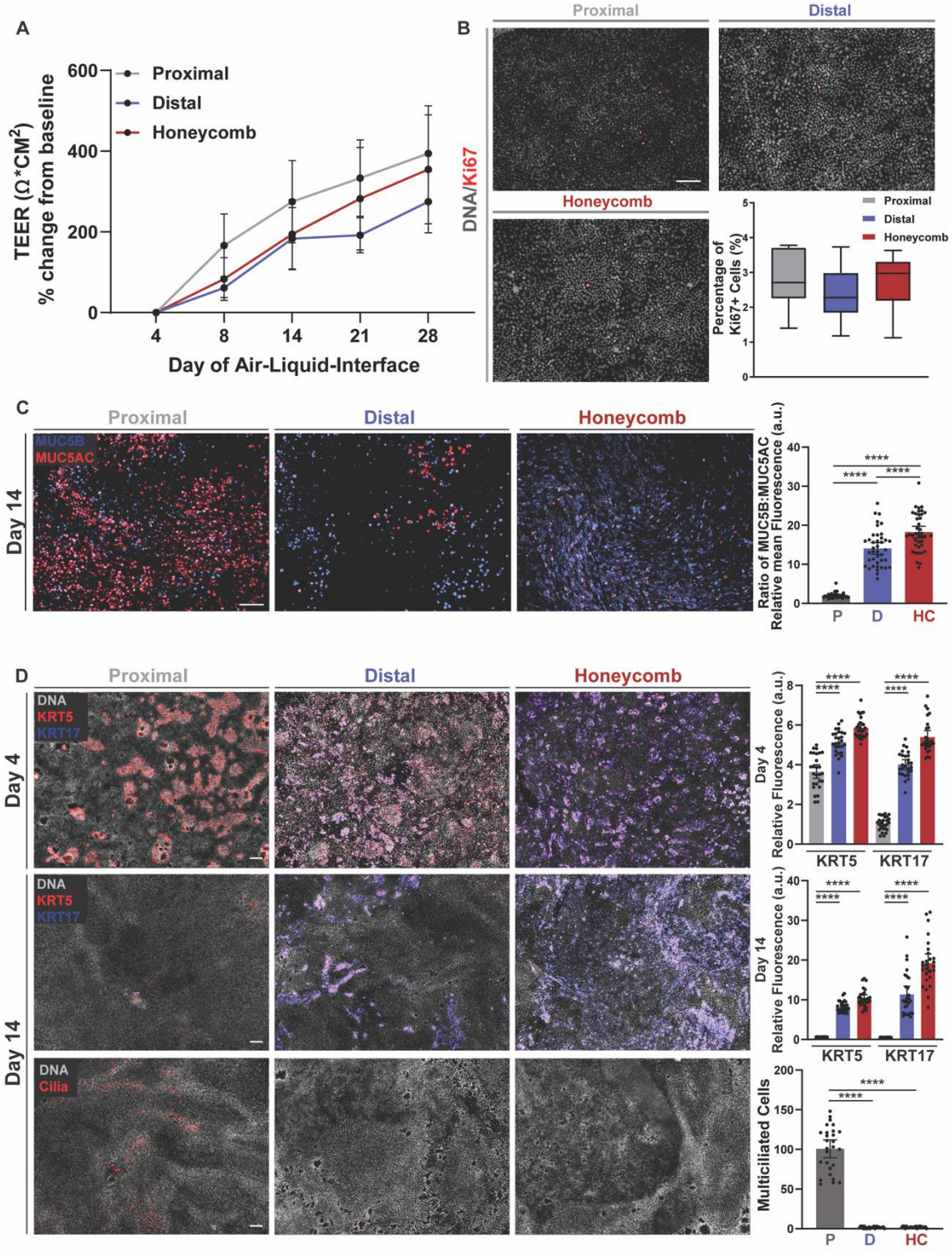


**Fig. S3. In vitro cultures recapitulate features of the IPF lung.** (**A**) Transepithelial electrical resistance (TEER) of culture proximal (P), distal (D), and honeycomb (HC) patient airway epithelia through air liquid-interface (ALI) differentiation. Error bars represent 95% confidence intervals. (**B**) Day 0 of ALI cultures stained for Ki67, a marker of proliferation, with

quantification of percentage of $Ki67^+$ cells. (**C**) Day 14 of ALI cultures stained for MUC5B/MUC5AC with quantification of the ratio $MUC5B^+$ to $MUC5AC^+$ in proximal (P), distal (D), and honeycomb cultures (HC). Error bars represent standard error of the mean (SEM). One-way ANOVA used for statistical comparison. (**D**) ALI cultures stained for KRT5 (day 4 and 14), KRT17 (day 4 and 14), acetylated tubulin (day 14) with quantification in proximal (P), distal (D), and honeycomb cultures (HC). Error bars represent SEM. One-way ANOVA used for statistical comparison. (A to D) For all statistical analysis ****$P<0.0001$. 100 μm scale bar shown. Epithelial culture experiments were independently performed $N \geq 3$ times with $n \geq 4$ donors.

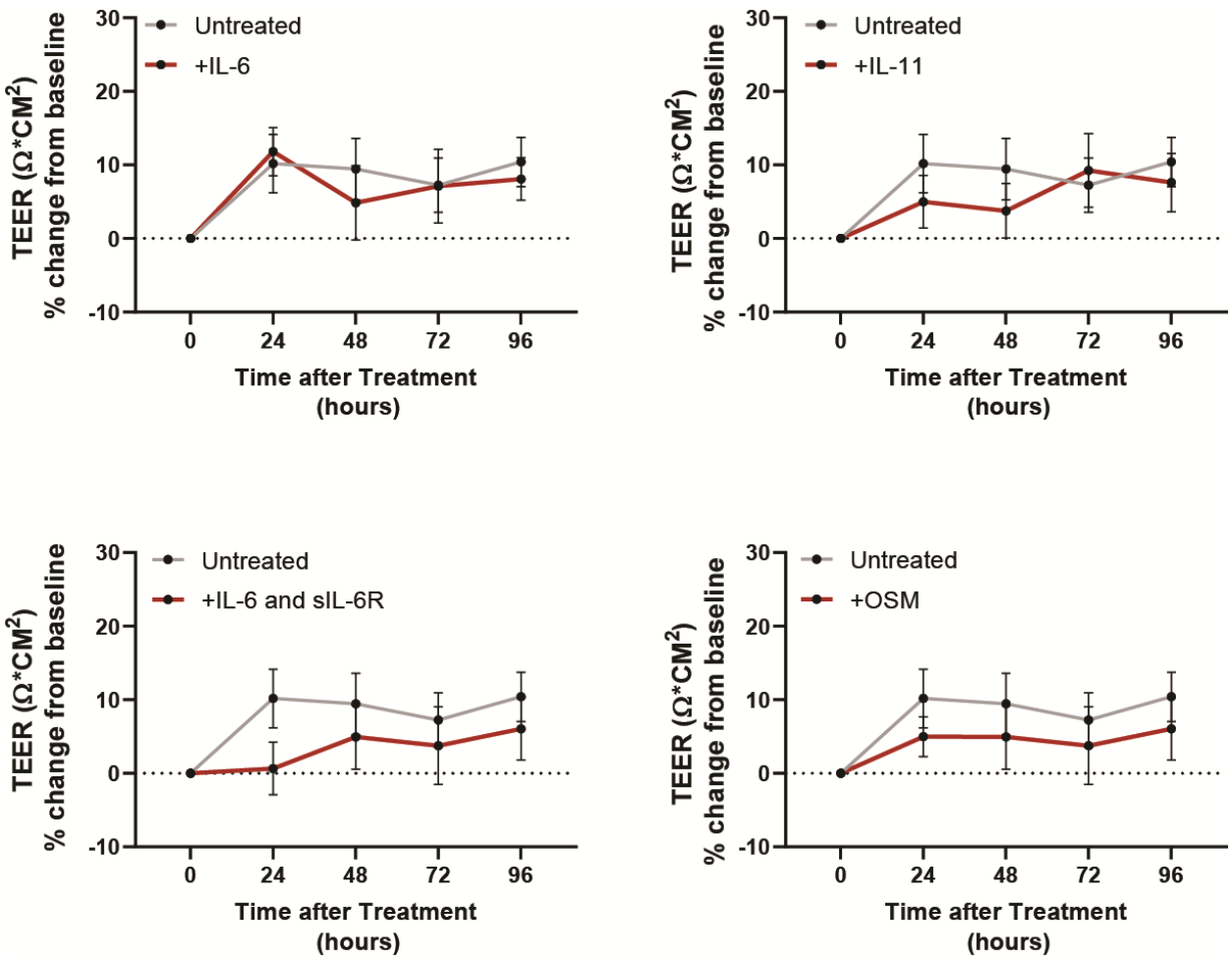


**Fig. S4. IL-6 family cytokine treatment does not alter epithelial barrier function.** Transepithelial electrical resistance (TEER) of IL-6 family cytokine stimulated cultures was measured every 24 hours after initial measurement/stimulation and followed for the extent of the culture period. Treatments shown are IL-6, IL-11, IL-6/sIL-6R, and OSM. Error bars represent 95% confidence interval. Epithelial culture experiments were independently performed $N \geq 3$ times with $n \geq 5$ donors.

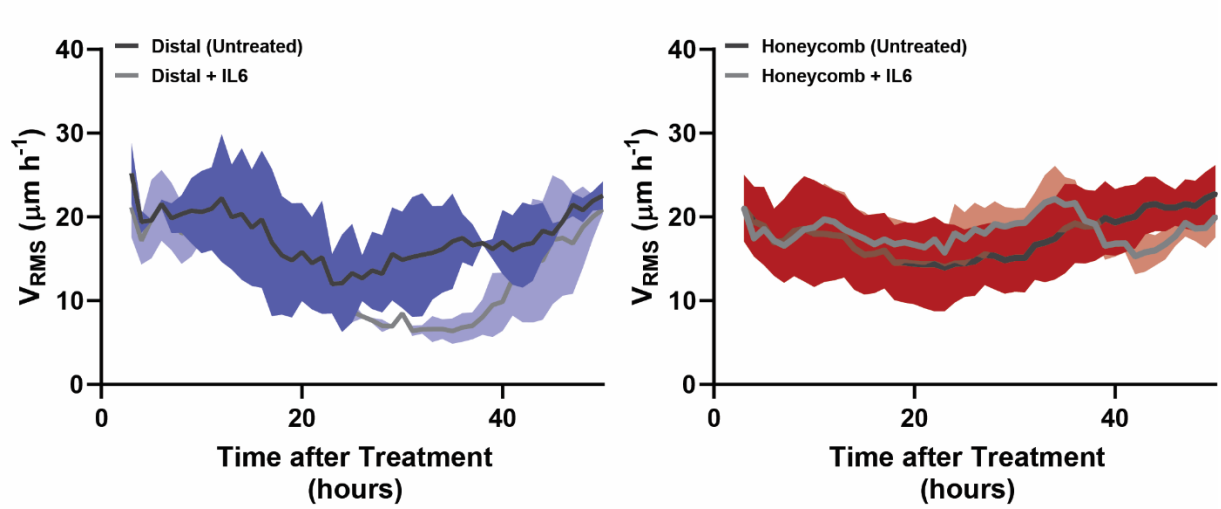


**Fig. S5. IL-6 treatment does not change dynamics in distal and honeycomb cultures.** Mean root mean-squared velocity ($V_{RMS}$) of distal and honeycomb culture for 48 hours after treatment with IL-6. Mean $V_{RMS}$ plotted with error bars representing 95% confidence intervals. Epithelial culture experiments were independently performed $N \geq 2$ times with $n \geq 4$ donors.

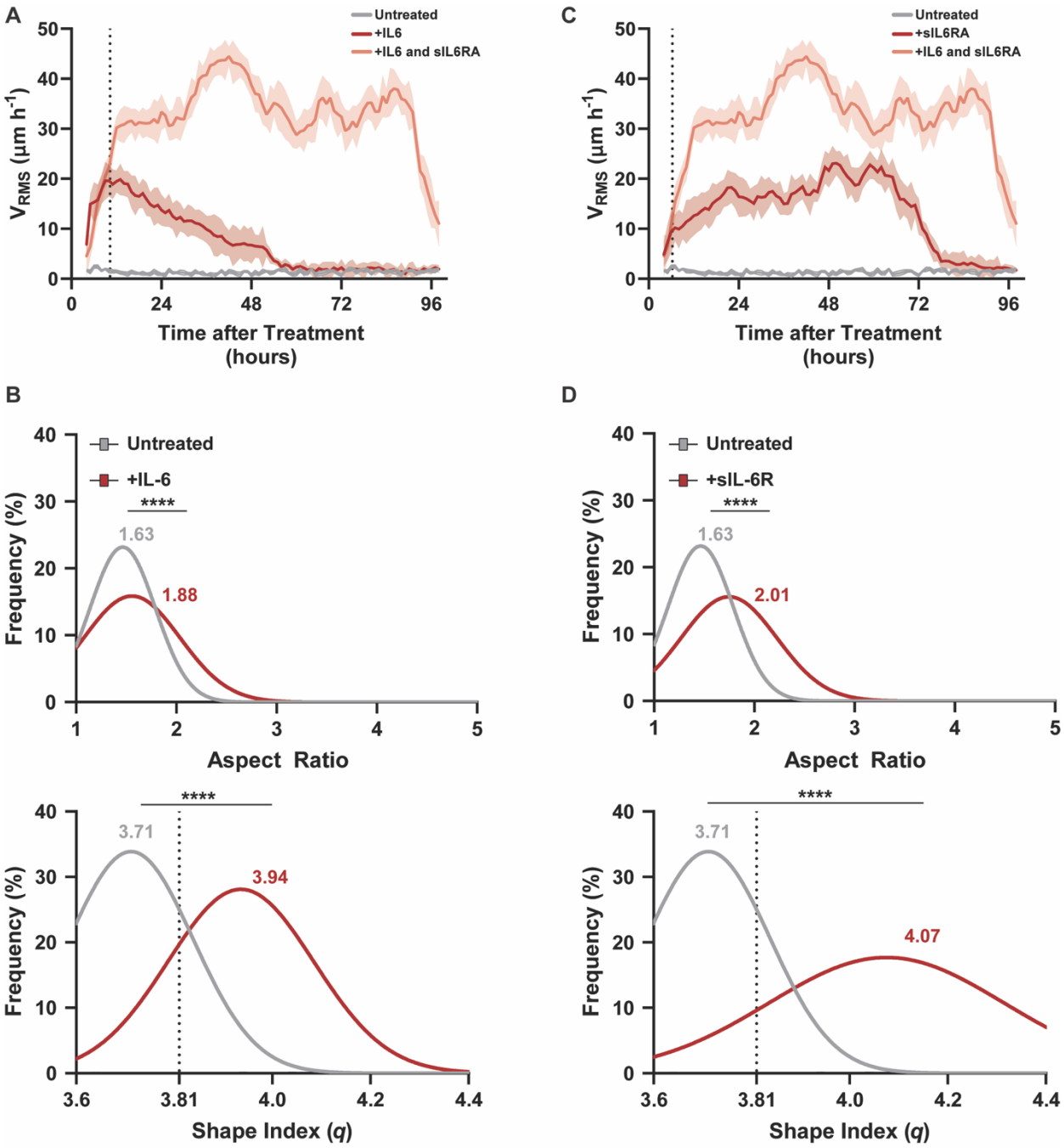


**Fig. S6. IL-6 or sIL-6Ra treatment alone is sufficient to induce fluidization.** (**A**) Mean root mean-squared velocity ($V_{RMS}$) of proximal culture stimulation with IL-6 or IL-6 and sIL-6Ra. Mean $V_{RMS}$ plotted with error bars representing 95% confidence intervals. Welch's t-test at each timepoint was used for statistical comparison.Dashed line represents time point (10.33 hours) after which treatments are statistically different. (**B**) Histogram of cellular aspect ratio (AR) and shape index (q) with mean values 24 hours after Il-6 stimulation. Cell-shape measurements were completed 24-hours after stimulation. Dashed line represents shape index of 3.81, the theoretical threshold between fluid and solid phases. One-way ANOVA was used for statistical comparison.

(**C**) Mean root mean-squared velocity ($V_{RMS}$) of proximal culture stimulation with sIL-6Ra or IL-6 and sIL-6Ra. Mean $V_{RMS}$ plotted with error bars representing 95% confidence intervals. Welch's *t*-test at each timepoint was used for statistical comparison. Dashed line represents time point (6.33 hours) after which treatments are statistically different. (**D**) Histogram of cellular aspect ratio (AR) and shape index (q) with mean values 24 hours after sIl-6Ra stimulation. Cell-shape measurements were completed 24-hours after stimulation. Dashed line represents shape index of 3.81, the theoretical threshold between fluid and solid phases. One-way ANOVA was used for statistical comparison. For all statistical analysis ****$P<0.0001$. Epithelial culture experiments were independently performed $N \geq 3$ times with $n \geq 5$ donors.

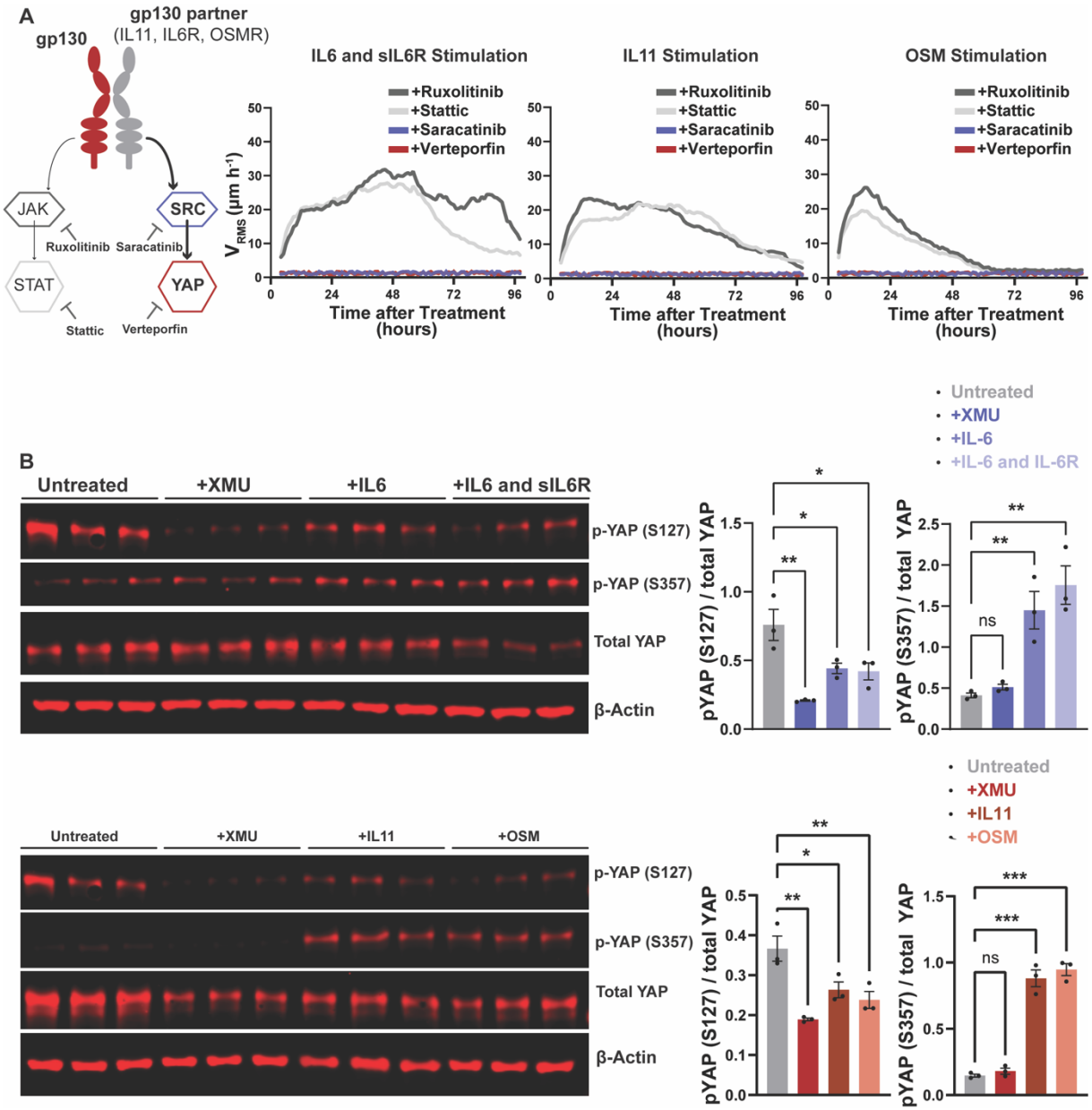


**Fig. S7. IL-6 family cytokine-induced fluidization is SRC/YAP dependent and leads to differential YAP phosphorylation.** (**A**) Left: treatment schema to determine JAK/STAT or SRC/YAP necessity in inducing epithelial fluidization via IL-6 family cytokine stimulation. Right: mean root mean-squared velocity ($V_{RMS}$) after co-treatment with IL-6 family cytokine (IL-6 and sIL-6RA, IL-11, or OSM) and either ruxolitinib (JAK1/2 inhibitor), stattic (STAT3 inhibitor), saracatanib (SRC inhibitor), or verteporforin (YAP inhibitor). (**B**) Western blot for YAP serine 127 (marker of targeting for degradation) and serine 357 (marker of nuclear localization) phosphorylation at 48 hours after stimulation. XMU shown as a positive control for decreased serine 127 phosphorylation. Error bars represent standard error of the mean. One-way ANOVA used for statistical comparison. Statistical analysis using one-way ANOVA. For all statistical analysis n.s. (not significant), *$P$<0.05, **$P$<0.01, ***$P$<0.001. Epithelial culture experiments were independently performed $N \geq 3$ times with $n \geq 5$ donors.

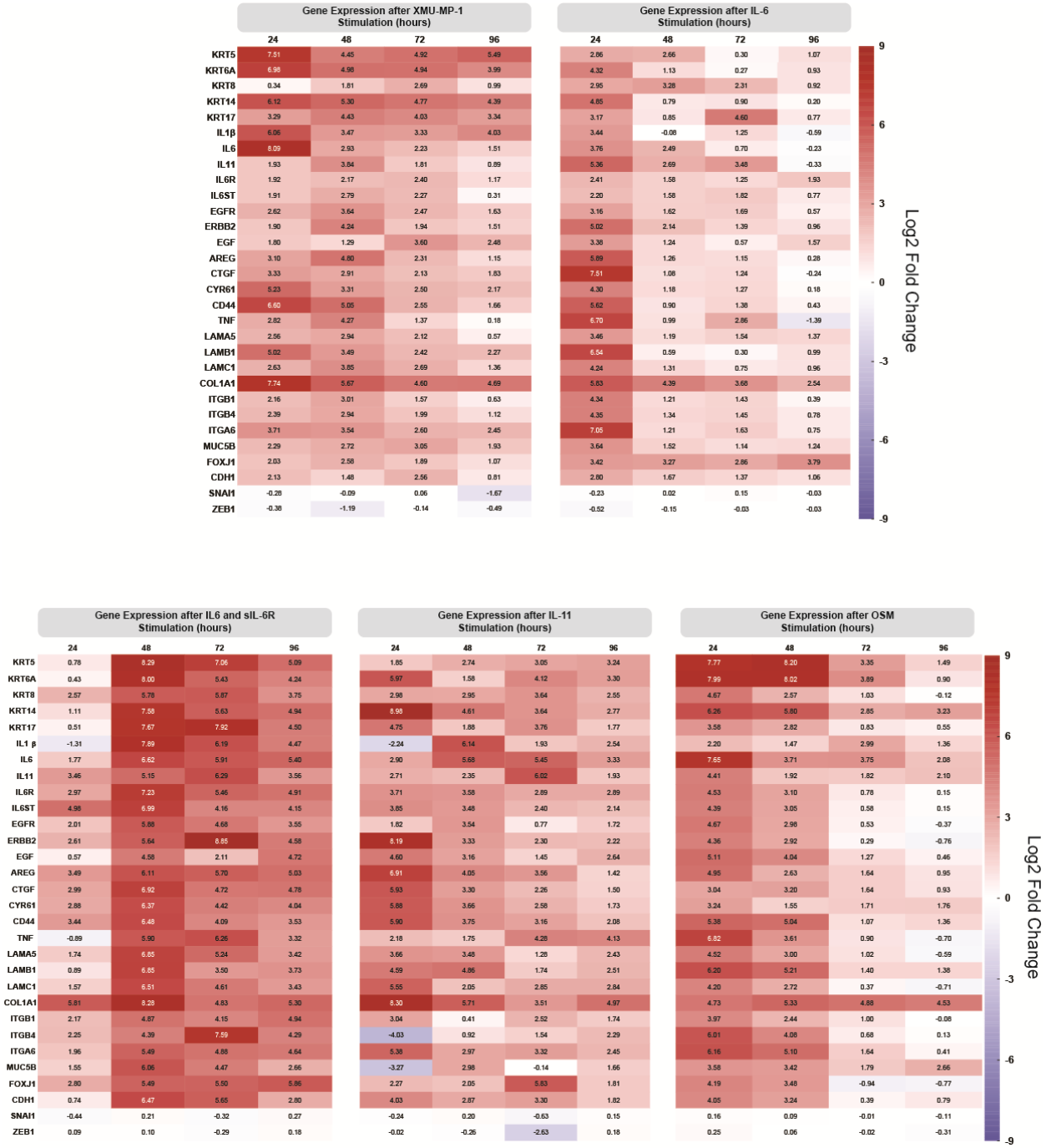


**Fig. S8. IPF-like gene signatures emerge after IL-6 family cytokine treatment.** Gene expression of IL-6 family cytokines stimulated proximal cultures every 24-hours after initial treatment. Transcript changes were determined by comparing stimulated culture gene expression to that of untreated cultures at the same time points. Shown are mean $\log_2$ fold change compared to untreated proximal cells at 24, 48, 72, and 96 hours. Epithelial culture experiments were independently performed $N = 4$ times with $n = 4$ donors.

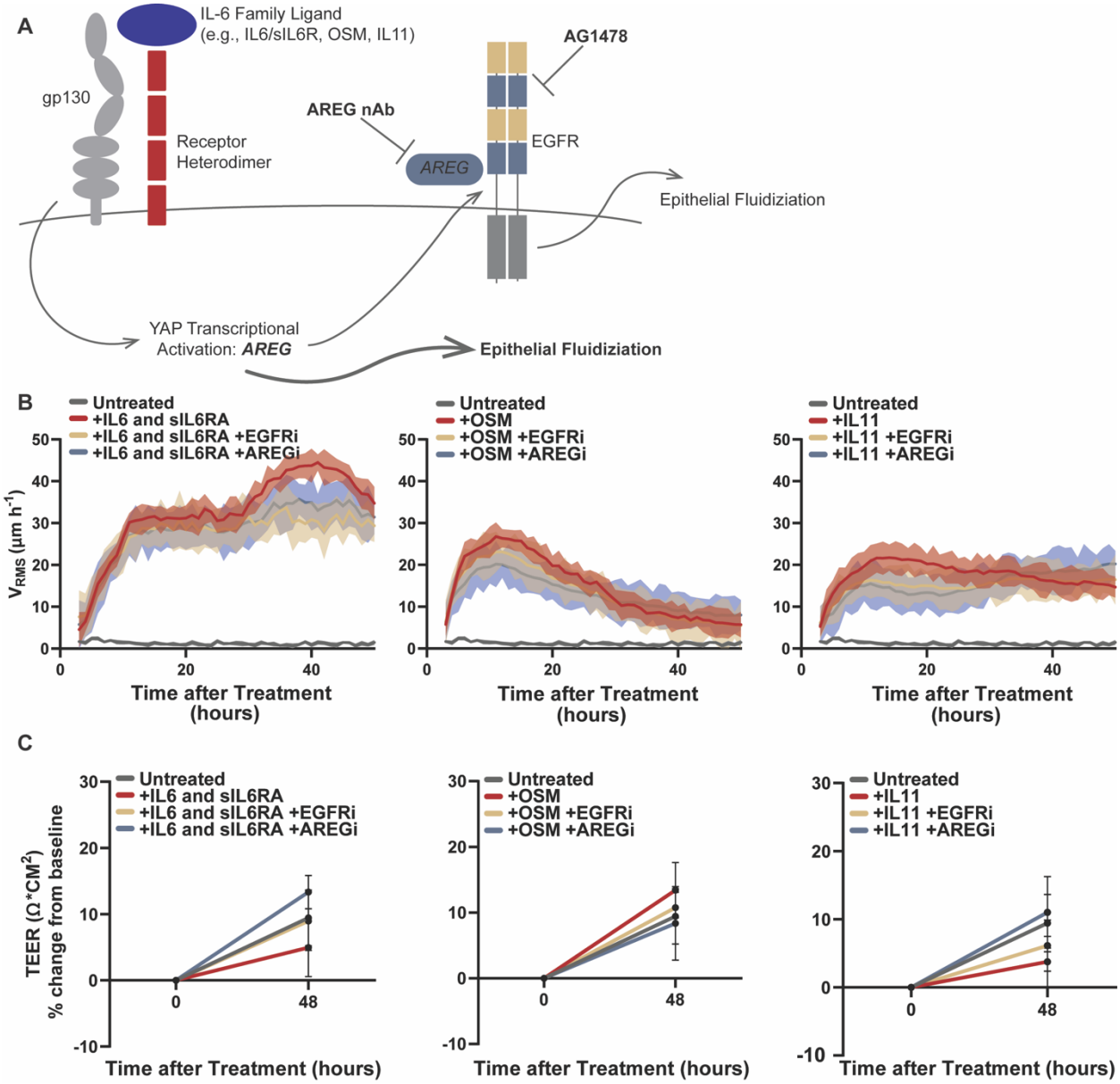


**Fig. S9. IL-6 family cytokine-induced fluidization is AREG-EGFR-independent.** (**A**) Schematic representing the possible crosstalk between IL-6 family cytokine stimulation and downstream activation of AREG-EGFR signaling with the corresponding inhibition regimen. (**B**) Mean root mean-squared velocity ($V_{RMS}$) for 48 hours after co-treatment with IL-6 family cytokine (IL-6 and sIL-6RA, OSM, or IL-11) and EGFR or AREG inhibitor. Mean $V_{RMS}$ plotted with error bars represent 95% confidence interval. (**C**) Transepithelial electrical resistance (TEER) of proximal cultures before and after IL-6 family cytokine stimulation and EGFR-related inhibition. Error bars represent 95% confidence interval. Epithelial culture experiments were independently performed $N = 3$ times with $n \geq 5$ donors.

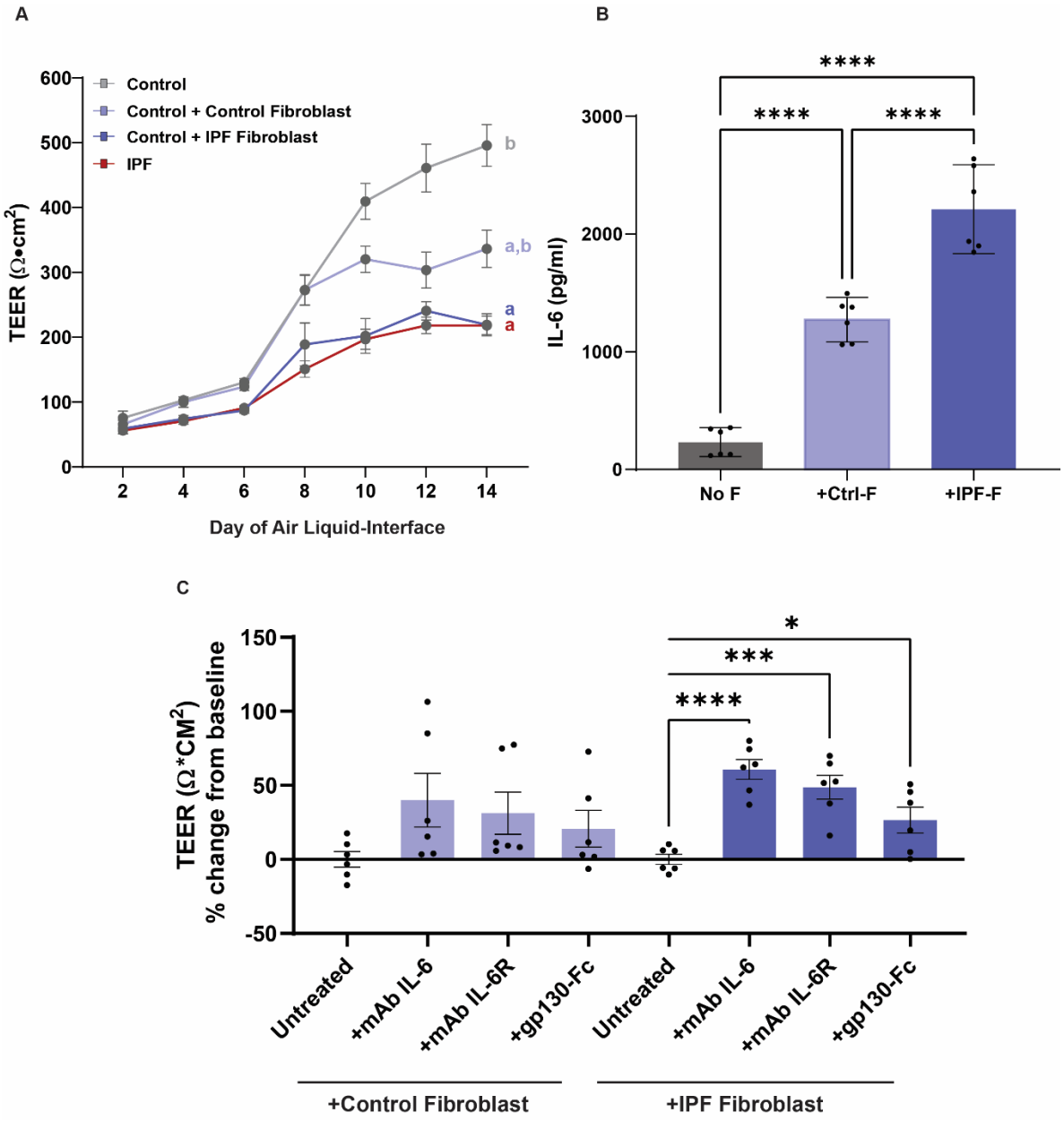


**Fig. S10. Co-culture systems diminish epithelial barrier function in a disease- and IL-6-dependent manner.** (**A**) Transepithelial electrical resistance (TEER) of control and IPF human lung fibroblast (HLF) co-culture with control epithelia from air-liquid interface (ALI) day 2 to 14. Additionally shown are control airway and IPF airway epithelial mono-cultures. Error bars represent 95% confidence intervals. One-way ANOVA was used for statistical comparisons with "a" representing statistical difference when compared to control monoculture and "b" representing statistical difference when compared to IPF monoculture. (**B**) IL-6 protein concentrations in control airway epithelial monoculture ("No F") and HLF co-culture conditions. Error bars represent 95% confidence interval. One-way ANOVA was used for statistical comparisons. (**C**) Percent change in baseline TEER of HLF co-cultures at ALI day 14 after continuous treatment with IL-6 cytokine family inhibitors (anti-IL-6 antibody, anti-IL-6R antibody, or gp130-Fc chimera). Error bars represent standard error of the mean. One-way

ANOVA used for statistical comparison. (A to C) For all statistical analysis *$P$<0.05, ***$P$<0.001, ****$P$<0.0001. Epithelial culture experiments were independently performed $N$ = 3 times with $n$ = 4 donors.

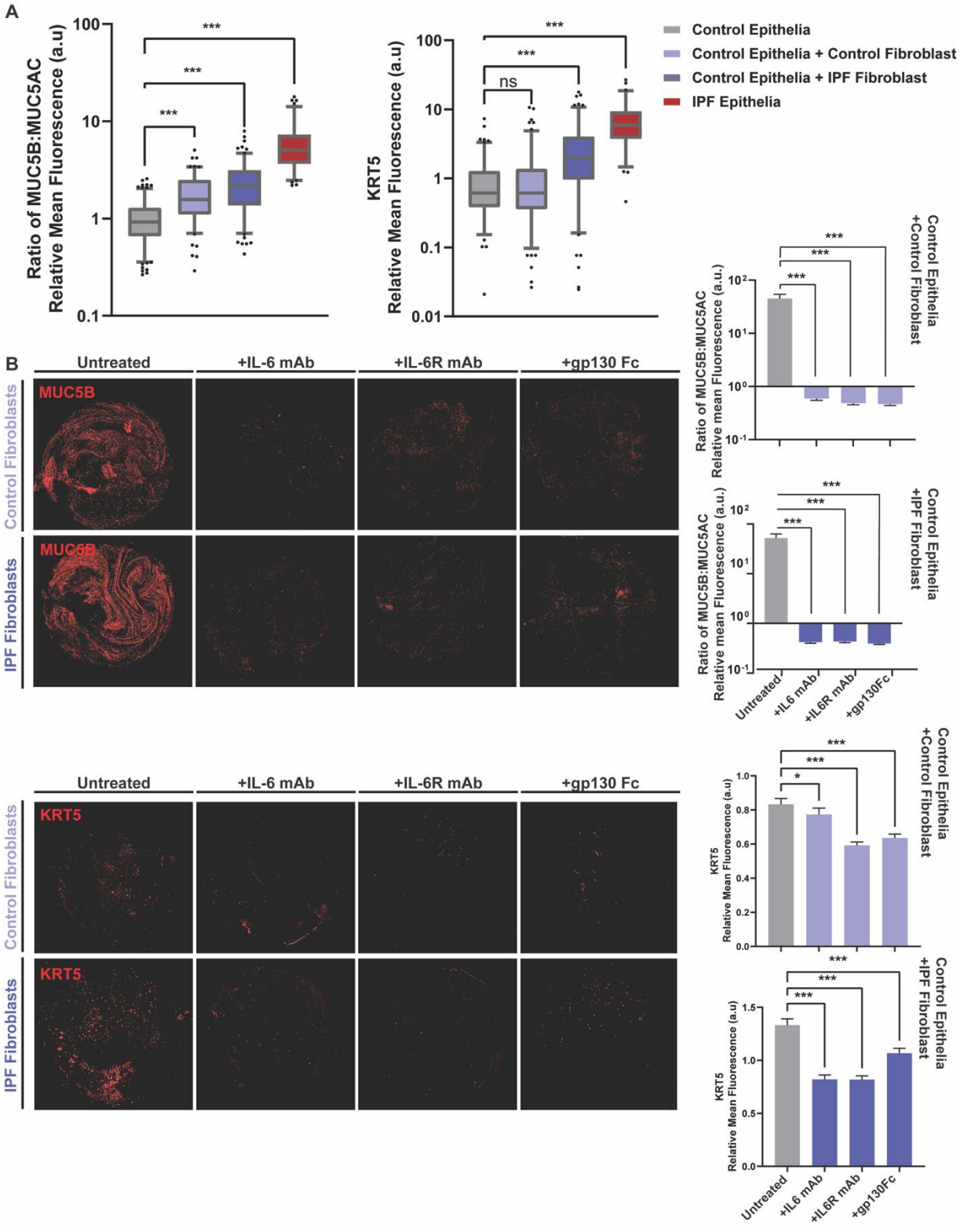


**Fig. S11. Co-culture systems increase MUC5B and KRT5 expression in an IL-6-dependent manner.** (**A**) Relative ratios of cell type markers in control airway and IPF airway mono-cultures compared to control and IPF human lung fibroblast (HLF) co-cultures. Shown are the ratio of

immunofluorescence of MUC5B to MUC5AC and KRT5 displayed as box plot of entire data range. One-way ANOVA used for statistical comparisons. (**B**) Representative images of MUC5B and KRT5 immunofluorescence in untreated cultures and cultures treated with IL-6 inhibitors. Quantification of the ratio of MUC5B to MUC5AC and KRT5 immunofluorescence for each treatment is shown. Error bars represent standard error of the mean. One-way ANOVA used for statistical comparisons. For all statistical analysis n.s. (not significant), *$P$<0.05, ***$P$<0.001. Epithelial culture experiments were independently performed $N$ = 3 times with $n$ = 4 donors.

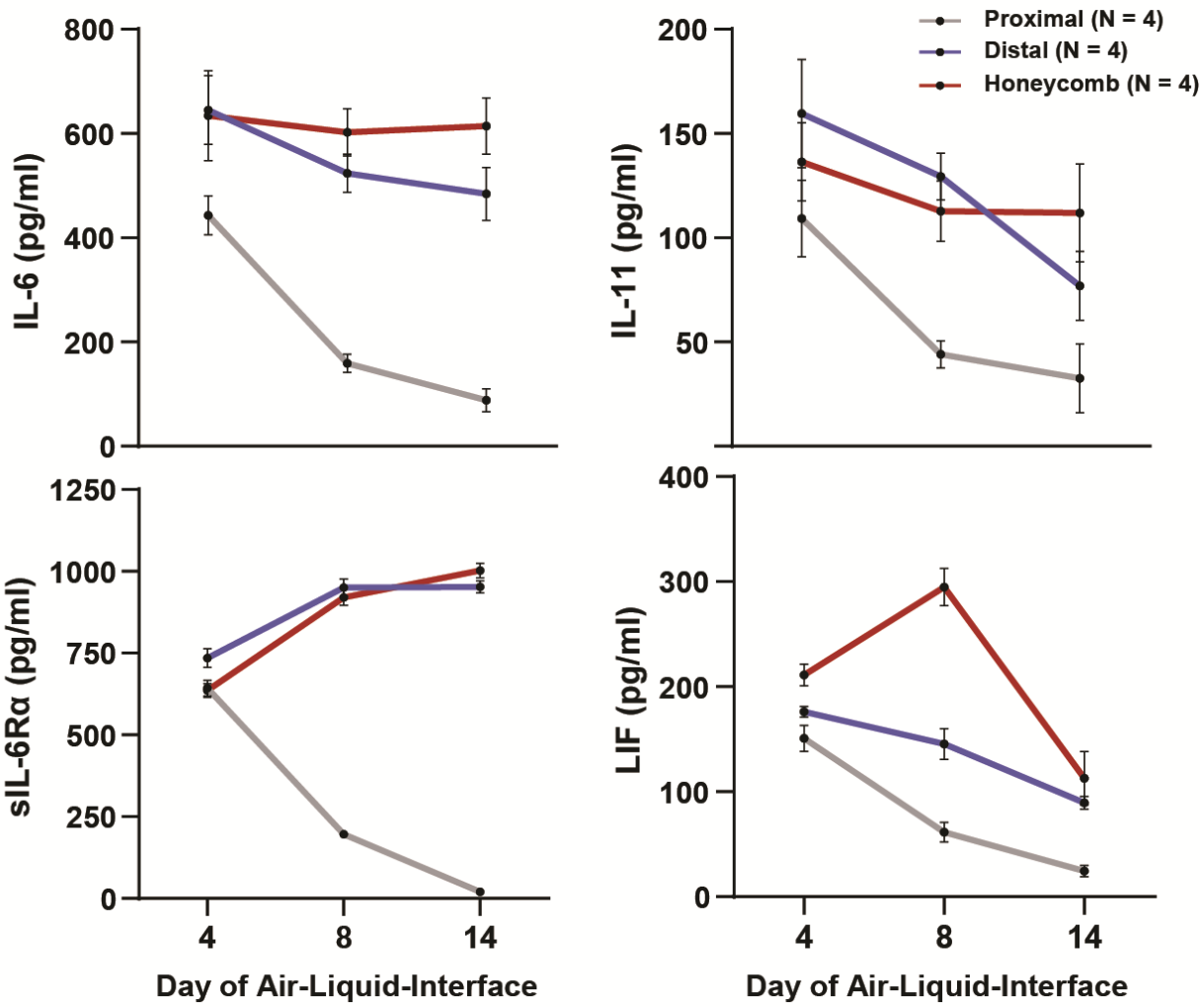


**Fig. S12. IL-6 family cytokines are increased in distal and honeycomb cultures.** Protein concentrations of IL-6 family cytokines from proximal, distal, and honeycomb cultures throughout air liquid-interface culture (days 4, 8 and 14). Cytokines shown are IL-6, IL-11, soluble IL-6 receptor (sIL-6Ra), and leukemia inhibitory factor (LIF). Error bars represent 95% confidence interval. Epithelial culture experiments were independently performed $N \geq 3$ times with $n \geq 4$ donors.

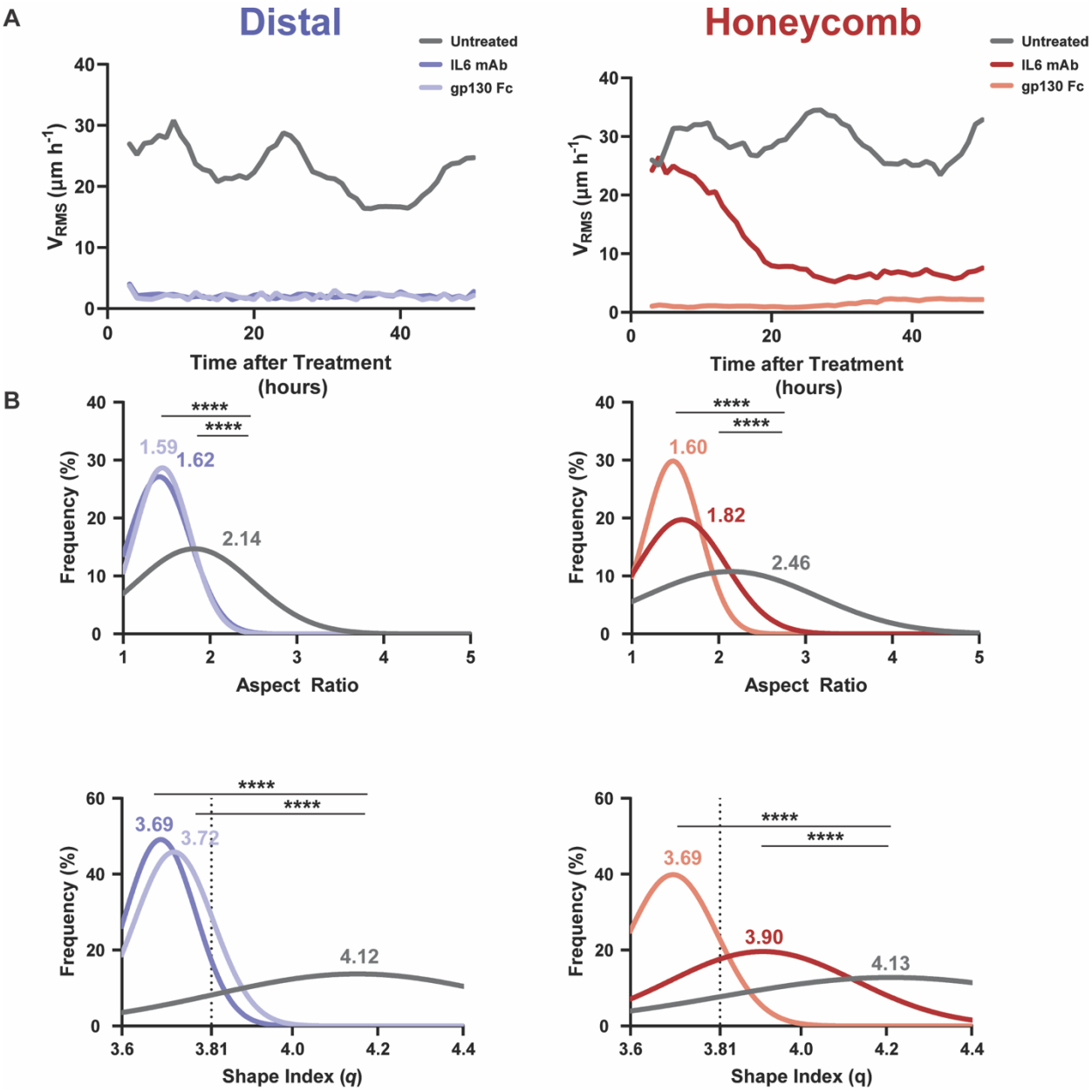


**Fig. S13. IL-6 signaling is required for persistent epithelial fluidization in distal and honeycomb cultures.** (**A**) Mean root mean-squared velocity ($V_{RMS}$) after distal or honeycomb cultures were treated with anti-IL-6 monoclonal antibody or gp130 Fc. (**B**) Histogram of cellular aspect ratio and shape index with mean values at 24 hours after inhibition. Dashed line represents shape index of 3.81, the theoretical threshold between fluid and solid phases. One-way ANOVA was used for statistical comparison. For all statistical analysis ****$P$<0.0001. Epithelial culture experiments were independently performed $N \geq 3$ times with $n \geq 4$ donors.

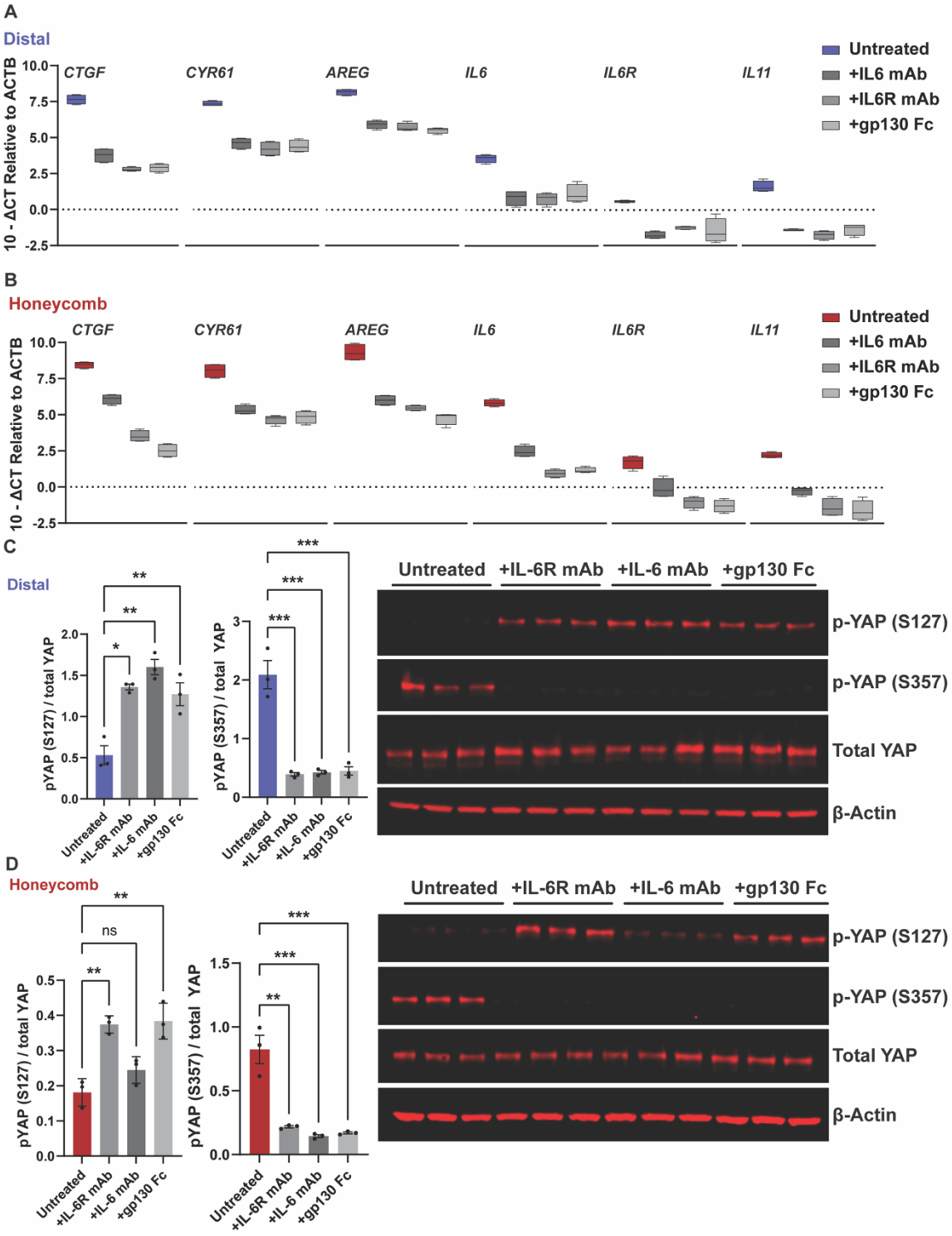


**Fig. S14. Inhibition of IL-6 signaling modifies gene expression and YAP phosphorylation state.** (**A**) Gene expression of distal airway epithelia treated with an anti-IL-6 antibody, anti-IL-6R antibody, or gp130-Fc chimera. Shown are box plots of entire data range. (**B**) Gene expression of honeycomb airway epithelia treated with an anti-IL-6 antibody, anti-IL-6R antibody, or gp130-Fc chimera. Shown are box plots of entire data range. (**C**) Western blot for

YAP serine 127 (marker of targeting for degradation) and serine 357 (marker of nuclear localization) phosphorylation at 48 hours after inhibition in distal cultures. Error bars represent standard error of the mean. One-way ANOVA was used for statistical comparison. (**D**) Western blot for YAP serine 127 (marker of targeting for degradation) and serine 357 (marker of nuclear localization) phosphorylation at 48 hours after inhibition in honeycomb cultures. Error bars represent standard error of the mean. One-way ANOVA was used for statistical comparison. (A to D) For all statistical analysis n.s. (not significant), $*P<0.05$, $**P<0.01$, $***P<0.001$. Epithelial culture experiments were independently performed $N \geq 3$ times with $n \geq 4$ donors.

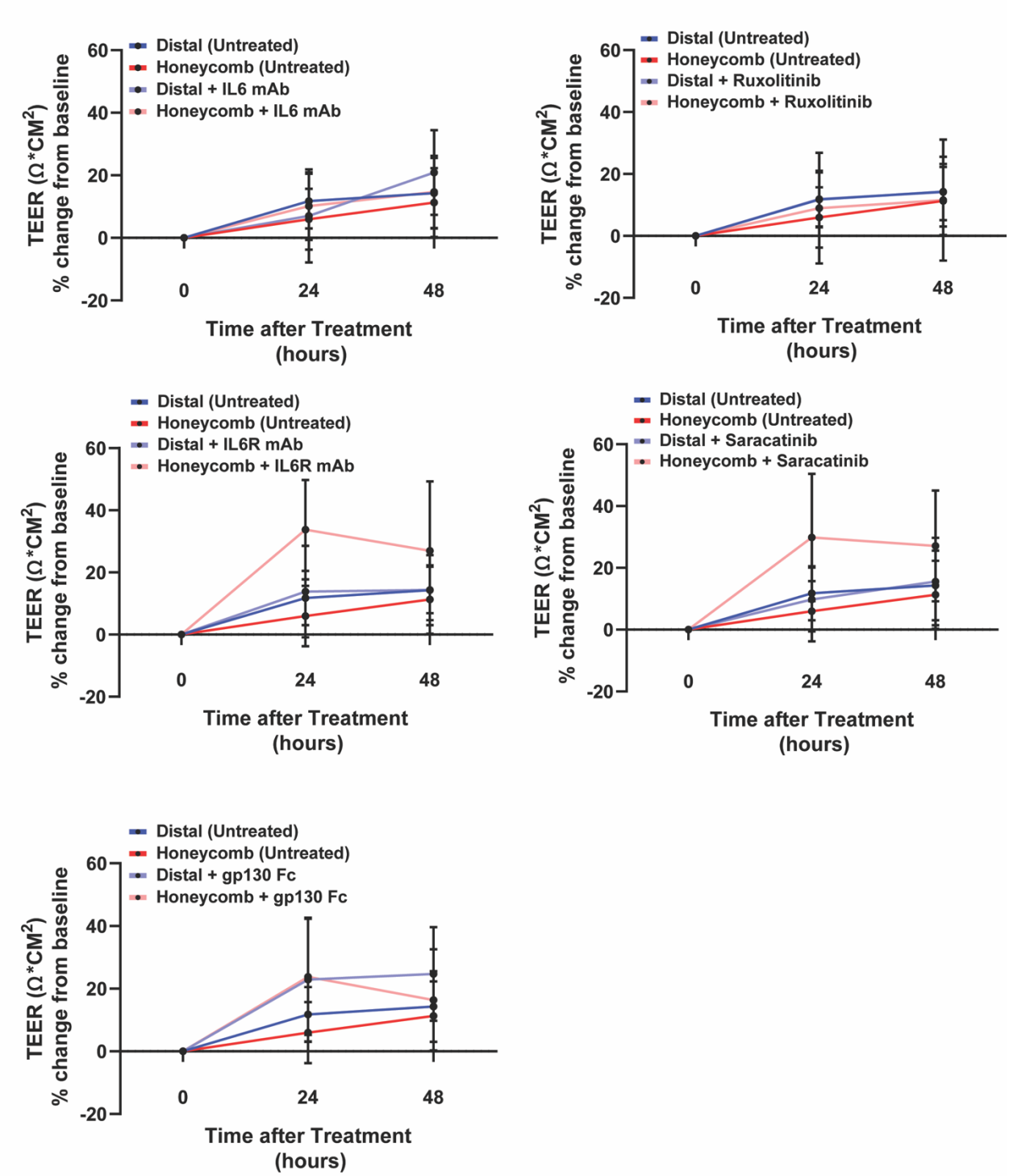


**Fig. S15. Epithelial barrier function is not compromised by IL-6-related inhibition.** Transepithelial electrical resistance (TEER) of distal or honeycomb cultures after inhibitor treatment. Error bars represent 95% confidence interval. Epithelial culture experiments were independently performed $N \geq 3$ times with $n \geq 4$ donors.

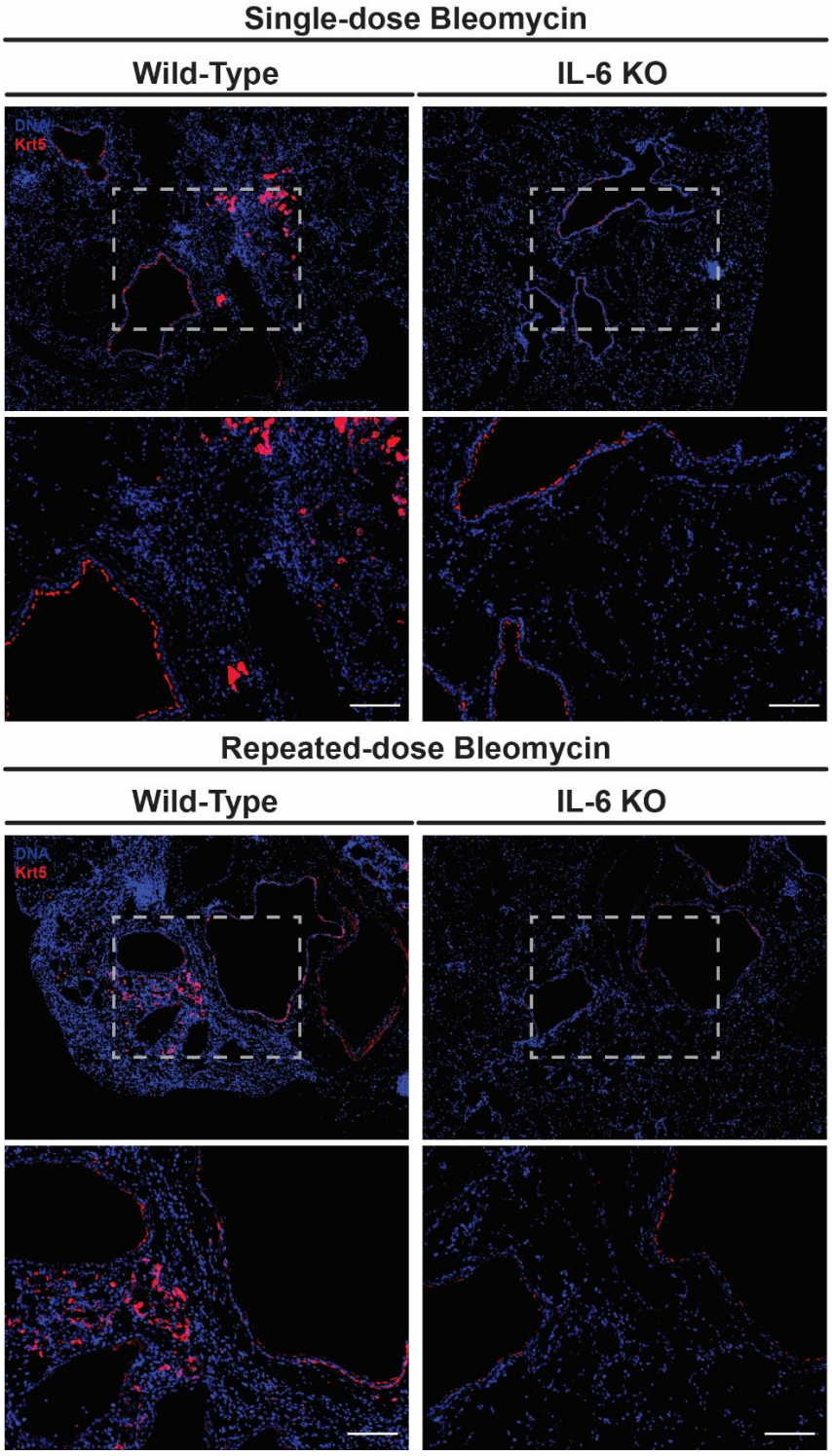


**Fig. S16. Bleomycin-induced Krt5$^+$ cells are present in airways but not parenchyma in IL-6 knockout mice.** Representative images of Krt5$^+$ cells in wild-type and IL-6 knockout (IL-6 KO) mice injured with either single-dose and repeated-dose bleomycin. Regions representing airways and parenchyma are shown. 100 μm scale bar shown.

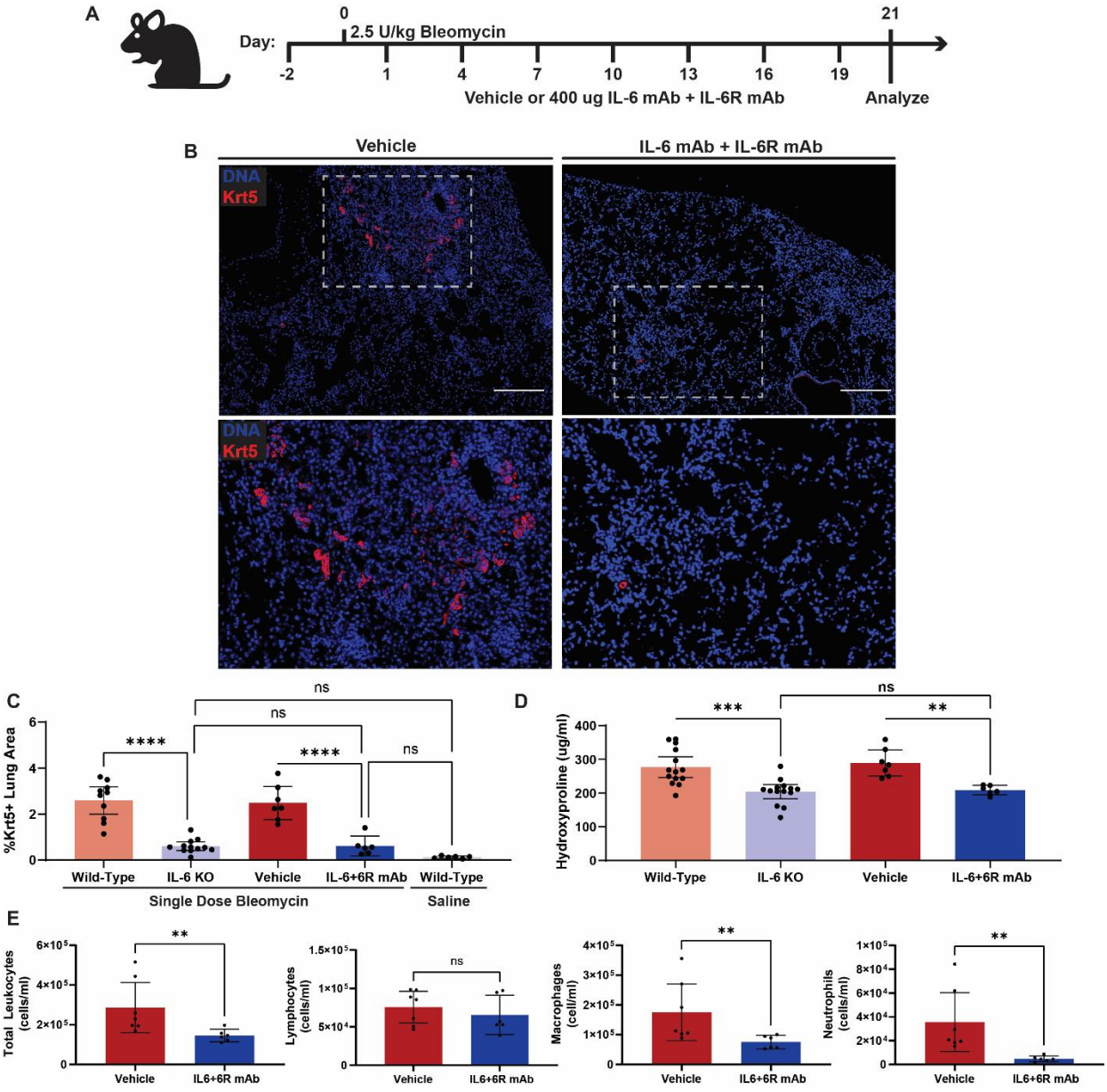


**Fig. S17. IL-6 and IL-6R pharmacologic inhibition protects mice from hallmarks of fibrotic lung injury. (A)** Dosing schematic for single-dose bleomycin exposure for wild-type mice treated with vehicle or combined anti-IL-6 and anti-IL-6R monoclonal antibodies (mAb). (**B**) Representative images of $Krt5^{+}$ staining in lungs of wild-type mice treated with vehicle or mAb. (**C**) Quantification of $Krt5^{+}$ area in the mouse lung after single-dose bleomycin for wild-type vehicle ($n$ = 7) or mAb treated ($n$ = 6) mice. Error bars represent 95% confidence interval. One-way ANOVA was used for statistical comparisons Single-dose bleomycin data for IL-6 knockout (IL-6 KO) re-graphed from Fig. 5E. (**D**) Quantification of hydroxyproline in the mouse lung after single-dose bleomycin for wild-type mice treated with vehicle ($n$ = 7) or mAb ($n$ = 6). Error bars represent 95% confidence interval. One-way ANOVA was used for statistical comparisons. Single-dose bleomycin data for IL-6 KO re-graphed from Fig. 5F. (**E**) Bronchoalveolar lavage fluid (BALF) cell counts from mice injured with single-dose bleomycin and treated with either vehicle or mAb. Quantified are counts for total leukocytes, macrophages, lymphocytes, and

neutrophils per milliliter of BALF. Error bars represent 95% confidence interval. Mann-Whitney test was used for statistical comparison. (A to E) For all statistical analysis n.s. (not significant), $^{**}P<0.01$, $^{***}P<0.001$, $^{****}P<0.0001$. 100 μm scale bar shown.

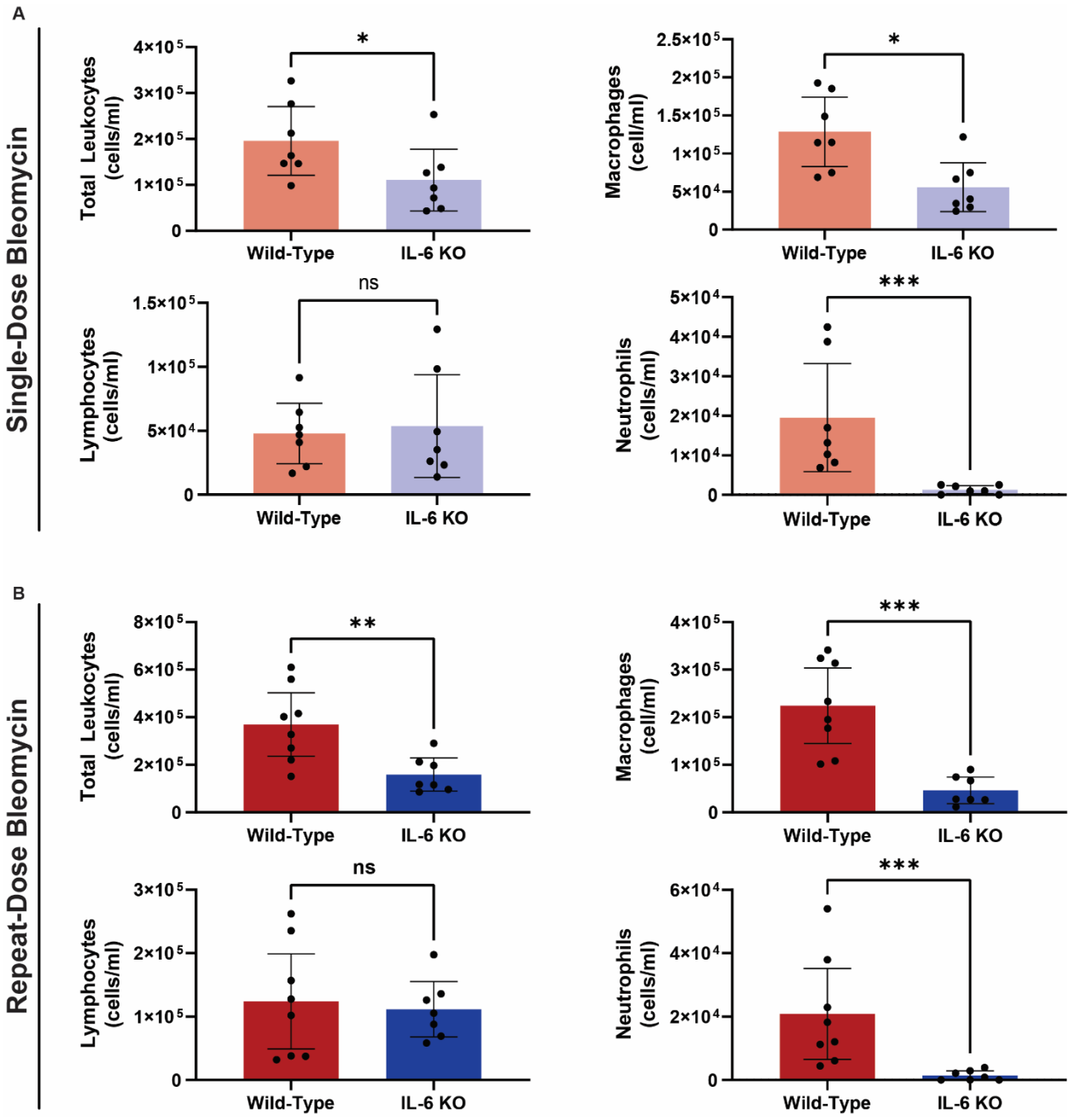


**Fig. S18. IL-6 deficiency changes bronchoalveolar leukocyte populations after bleomycin-induced lung injury.** (**A**) Bronchoalveolar lavage fluid (BALF) cell counts from mice injured with single-dose bleomycin 21 days after initial injury (wild-type: $n = 7$, IL-6 KO: $n = 7$). (**B**) BALF cell counts from mice injured with repeated-dose bleomycin 49 days after initial injury (wild-type: $n = 8$, IL-6 KO: $n = 7$). (A and B) Quantified are counts for total leukocytes, macrophages, lymphocytes, and neutrophils per milliliter of BALF. Error bars represent 95% confidence interval. Mann-Whitney test was used for statistical comparison. For all statistical analysis n.s. (not significant), $*P<0.05$, $**P<0.01$, $***P<0.001$.

**Table S1. Primary cell donor information.** List of: cell type, anatomical region where the cells were isolated from, passage used for experimentation, age, sex, smoking history, *MUC5B* variant status, and disease status.

| Cell-type | Anatomic region | Passage | Age | Sex | Smoking | Variant Status | Disease Status |
|---|---|---|---|---|---|---|---|
| Epithelial | Proximal | 2 | 63.5 ±4.2 | 6 M | Never (4) : Ever (2) | 3 GG : 3 GT | IPF |
| | Distal | 2 | | | | | |
| | Honeycomb | 2 | | | | | |
| | Distal | 2 | 61.3 ±4.0 | 2 M : 1 F | Never (2) : Ever (1) | 3 GG | Control |
| Fibroblast | Parenchyma | 3 | 58.8 ±4.4 | 2 M: 2 F | Never (2) : Ever (2) | 4 GG | Control |
| | | 3 | 67.6 ±0.6 | 2 M: 1 F | Never (2) : Ever (1) | 2 GG: 1 GT | IPF |

**Table S2. Genes differentially regulated in regional epithelial cultures.** List of conserved genes that down regulated in proximal cultures transitioning from a fluid-like to solid-like phase, and persistently upregulated in distal and honeycomb epithelial cultures compared to proximal non-migratory cultures. Shown are log2foldchange and adjusted *P*-value.

| | Distal | | Honeycomb | | Proximal | |
|---|---|---|---|---|---|---|
| Gene | L2FC | $P_{adj}$ | L2FC | $P_{adj}$ | L2FC | $P_{adj}$ |
| A2ML1 | 1.04 | 9.53E-04 | 3.45 | 1.29E-03 | -4.17 | 1.18E-20 |
| AAK1 | 0.26 | 7.02E-02 | 0.22 | 3.74E-02 | -0.47 | 4.06E-02 |
| ABCA7 | 0.52 | 6.95E-11 | 0.75 | 4.12E-08 | -0.51 | 6.36E-03 |
| ABL2 | 0.30 | 2.24E-02 | 0.51 | 2.46E-05 | -0.88 | 3.27E-03 |
| AC008870.1 | 0.64 | 2.30E-08 | 0.59 | 9.02E-05 | -0.61 | 2.06E-10 |
| AC011043.1 | 1.78 | 8.77E-02 | 1.82 | 2.38E-04 | -1.84 | 1.06E-03 |
| AC016582.3 | 1.45 | 1.04E-04 | 2.07 | 1.30E-04 | -1.10 | 4.74E-02 |
| AC025580.1 | 3.19 | 1.46E-04 | 4.40 | 2.92E-16 | -5.67 | 2.63E-07 |
| AC025580.2 | 1.25 | 2.48E-02 | 2.10 | 1.17E-04 | -2.77 | 1.48E-03 |
| AC026877.1 | 0.61 | 1.18E-03 | 0.52 | 1.90E-02 | -0.43 | 3.87E-02 |
| AC048382.5 | 1.65 | 4.22E-02 | 1.81 | 8.23E-03 | -1.17 | 4.18E-02 |
| AC092117.1 | 2.12 | 2.29E-05 | 2.06 | 1.13E-03 | -1.62 | 7.14E-03 |
| AC098614.4 | 0.63 | 1.35E-02 | 0.63 | 1.62E-02 | -0.73 | 2.98E-02 |
| AC116050.1 | 2.79 | 3.03E-11 | 3.00 | 3.66E-09 | -2.25 | 1.06E-02 |
| AC121764.1 | 3.36 | 2.07E-05 | 4.48 | 8.58E-12 | -2.07 | 9.16E-03 |
| AC126755.1 | 1.10 | 1.07E-12 | 0.95 | 2.16E-05 | -0.64 | 4.46E-02 |
| AC126755.2 | 1.06 | 1.35E-02 | 0.89 | 8.32E-02 | -1.00 | 1.77E-02 |
| AC138969.2 | 3.34 | 1.56E-05 | 2.80 | 1.16E-03 | -1.19 | 1.83E-02 |
| AC145212.1 | 1.54 | 5.91E-15 | 1.84 | 3.76E-17 | -0.92 | 3.73E-02 |
| AC215219.1 | 1.20 | 8.54E-16 | 1.37 | 2.40E-13 | -1.15 | 7.30E-06 |
| AC231533.2 | 1.88 | 9.78E-04 | 2.00 | 7.70E-04 | -1.55 | 2.48E-04 |
| AC244153.1 | 1.06 | 1.70E-07 | 0.77 | 5.36E-03 | -0.75 | 1.28E-05 |
| AC245041.1 | 2.06 | 1.07E-04 | 1.99 | 6.07E-14 | -0.99 | 2.37E-06 |
| ACAA2 | 1.24 | 3.16E-06 | 1.63 | 5.78E-15 | -1.32 | 9.97E-10 |
| ACTA2 | 1.27 | 1.25E-03 | 1.46 | 2.37E-07 | -2.33 | 2.38E-09 |
| ACTB | 0.44 | 1.40E-06 | 0.71 | 5.32E-17 | -0.73 | 8.89E-03 |
| ACTG1 | 0.34 | 1.92E-03 | 0.56 | 1.16E-09 | -0.66 | 1.67E-02 |
| ACTN4 | 0.18 | 2.82E-02 | 0.28 | 1.19E-03 | -0.49 | 5.46E-05 |
| ADA | 0.83 | 9.70E-03 | 0.98 | 9.63E-07 | -1.29 | 2.15E-03 |
| ADRA2B | 6.77 | 1.07E-02 | 6.60 | 5.57E-03 | -5.33 | 2.41E-03 |
| ADRB2 | 0.49 | 3.82E-03 | 0.98 | 1.74E-09 | -0.54 | 5.60E-06 |
| AGPAT5 | 0.29 | 3.03E-02 | 0.23 | 6.90E-02 | -0.48 | 3.91E-03 |
| AK4 | 0.40 | 2.97E-02 | 0.38 | 7.47E-03 | -0.64 | 8.55E-03 |
| ALAS1 | 0.20 | 1.82E-02 | 0.45 | 9.45E-03 | -0.33 | 3.82E-03 |
| ALDH1A2 | 2.14 | 1.10E-04 | 3.08 | 1.99E-10 | -1.31 | 4.61E-03 |
| ALDH1B1 | 0.25 | 6.83E-02 | 0.43 | 1.16E-03 | -0.77 | 3.55E-02 |
| ALOX5 | 3.80 | 7.06E-29 | 4.01 | 6.66E-41 | -2.45 | 2.31E-02 |
| ALPP | 3.38 | 4.16E-02 | 4.69 | 1.09E-04 | -5.29 | 9.68E-06 |
| ANGEL1 | 0.34 | 3.37E-02 | 0.43 | 3.08E-03 | -0.24 | 2.44E-02 |
| ANKDD1A | 2.25 | 9.68E-07 | 1.36 | 1.03E-02 | -1.63 | 9.20E-03 |

| | | | | | | |
|---|---|---|---|---|---|---|
| ANKLE2 | 0.35 | 1.59E-04 | 0.58 | 2.74E-08 | -0.73 | 4.42E-04 |
| ANKRD11 | 0.20 | 6.17E-02 | 0.23 | 5.42E-02 | -0.32 | 1.08E-03 |
| ANO5 | 1.88 | 5.37E-02 | 2.53 | 4.97E-03 | -2.62 | 1.28E-03 |
| ANXA3 | 0.71 | 4.05E-10 | 1.29 | 4.37E-26 | -1.58 | 4.35E-04 |
| ANXA8 | 0.50 | 7.41E-02 | 0.59 | 6.83E-06 | -0.72 | 7.97E-03 |
| AP005403.1 | 2.11 | 9.76E-03 | 1.96 | 5.30E-02 | -1.95 | 1.30E-03 |
| APBA1 | 0.82 | 5.27E-03 | 1.34 | 2.93E-06 | -0.95 | 7.34E-08 |
| APBA2 | 1.19 | 1.55E-05 | 1.80 | 5.57E-21 | -0.83 | 1.17E-02 |
| APH1B | 0.49 | 2.20E-02 | 0.63 | 2.52E-05 | -0.39 | 3.15E-02 |
| APOBEC3C | 0.99 | 1.19E-09 | 0.69 | 8.94E-07 | -0.85 | 9.16E-30 |
| APOBEC3G | 0.66 | 2.41E-03 | 0.52 | 8.84E-03 | -0.64 | 5.62E-04 |
| APOE | 1.18 | 1.11E-04 | 1.70 | 3.41E-12 | -2.38 | 1.35E-13 |
| AREG | 0.51 | 3.13E-02 | 1.32 | 2.77E-08 | -0.87 | 2.65E-02 |
| ARFRP1 | 0.25 | 2.84E-02 | 0.35 | 1.62E-03 | -0.40 | 1.04E-02 |
| ARHGAP10 | 0.56 | 1.45E-03 | 0.54 | 5.92E-04 | -0.81 | 7.15E-10 |
| ARHGAP8 | 0.49 | 6.45E-05 | 0.65 | 8.35E-07 | -0.84 | 8.84E-06 |
| ARHGEF18 | 0.26 | 2.79E-03 | 0.42 | 1.14E-06 | -0.47 | 7.29E-04 |
| ARHGEF2 | 0.18 | 8.19E-02 | 0.42 | 8.37E-05 | -0.62 | 1.21E-05 |
| ARHGEF39 | 1.28 | 1.64E-03 | 1.28 | 1.56E-03 | -1.41 | 5.15E-08 |
| ARID3A | 0.46 | 9.30E-03 | 0.71 | 1.01E-04 | -1.02 | 3.08E-05 |
| ARL16 | 0.46 | 7.76E-05 | 0.45 | 1.78E-03 | -0.39 | 1.73E-03 |
| ARL6IP5 | 0.42 | 2.25E-10 | 0.53 | 1.45E-12 | -0.54 | 2.15E-04 |
| ARNTL2 | 0.24 | 9.44E-03 | 0.37 | 4.04E-03 | -0.45 | 2.16E-04 |
| ARPC5L | 0.26 | 3.71E-04 | 0.36 | 2.18E-03 | -0.20 | 2.07E-02 |
| ASAP1 | 0.27 | 4.17E-02 | 0.47 | 6.51E-04 | -0.76 | 3.37E-04 |
| ASL | 0.19 | 9.42E-02 | 0.39 | 6.06E-04 | -0.32 | 2.76E-02 |
| ATG10 | 0.77 | 9.12E-04 | 0.91 | 2.25E-04 | -0.74 | 1.49E-03 |
| ATP11A | 0.52 | 1.21E-11 | 0.65 | 1.43E-09 | -0.38 | 1.23E-04 |
| ATP13A4 | 0.95 | 2.91E-05 | 1.74 | 2.38E-28 | -1.18 | 6.11E-10 |
| ATP6V1B2 | 0.30 | 3.01E-04 | 0.36 | 5.89E-04 | -0.40 | 2.17E-06 |
| ATXN2 | 0.20 | 8.02E-02 | 0.39 | 8.22E-04 | -0.29 | 4.12E-02 |
| B4GALNT4 | 1.58 | 6.77E-09 | 1.81 | 3.98E-11 | -1.33 | 2.16E-04 |
| BAK1 | 0.31 | 9.72E-02 | 0.36 | 6.61E-03 | -0.49 | 7.11E-16 |
| BCL2A1 | 1.76 | 7.03E-06 | 2.81 | 5.56E-14 | -2.69 | 4.93E-06 |
| BMP2 | 0.38 | 1.57E-02 | 0.41 | 4.19E-02 | -0.77 | 1.02E-02 |
| BPHL | 0.40 | 1.01E-02 | 0.46 | 3.56E-03 | -0.36 | 2.03E-03 |
| BRI3 | 0.30 | 7.91E-04 | 0.49 | 4.95E-04 | -0.26 | 2.51E-02 |
| BTBD2 | 0.31 | 3.63E-04 | 0.30 | 2.39E-03 | -0.34 | 2.54E-05 |
| BTN3A2 | 2.44 | 2.91E-67 | 2.44 | 3.91E-104 | -1.45 | 3.89E-02 |
| BZW2 | 0.35 | 2.37E-04 | 0.26 | 3.54E-02 | -0.31 | 1.84E-03 |
| C15orf48 | 0.84 | 2.27E-11 | 1.56 | 3.23E-05 | -1.48 | 5.80E-04 |
| C19orf48 | 0.41 | 9.31E-06 | 0.44 | 4.16E-05 | -0.39 | 5.28E-05 |
| C2orf54 | 0.96 | 1.39E-04 | 1.01 | 1.72E-06 | -1.19 | 2.57E-09 |
| C3orf52 | 0.37 | 8.38E-03 | 0.49 | 9.29E-04 | -0.71 | 1.24E-04 |
| C9orf40 | 0.41 | 3.93E-02 | 0.44 | 7.00E-02 | -0.52 | 1.28E-04 |
| CA7 | 2.58 | 7.18E-02 | 2.59 | 2.26E-03 | -2.81 | 1.35E-03 |
| CACUL1 | 0.23 | 2.66E-02 | 0.24 | 3.65E-02 | -0.26 | 1.85E-04 |
| CALM3 | 0.20 | 2.81E-02 | 0.26 | 4.36E-03 | -0.35 | 4.47E-02 |
| CAP1 | 0.22 | 2.75E-02 | 0.36 | 8.98E-06 | -0.41 | 1.82E-02 |

| | | | | | | |
|---|---|---|---|---|---|---|
| CAPG | 0.38 | 1.95E-03 | 0.37 | 1.80E-02 | -0.64 | 2.80E-08 |
| CAPN12 | 1.26 | 1.86E-02 | 1.09 | 1.85E-05 | -1.47 | 2.26E-07 |
| CAPN14 | 0.93 | 5.17E-03 | 1.86 | 3.02E-02 | -1.33 | 2.56E-02 |
| CAPNS2 | 0.99 | 1.10E-04 | 0.93 | 4.02E-05 | -0.68 | 2.32E-05 |
| CARD10 | 0.87 | 3.96E-05 | 1.30 | 5.70E-11 | -1.53 | 3.57E-15 |
| CARD11 | 0.61 | 7.78E-04 | 0.77 | 2.39E-09 | -0.76 | 9.83E-04 |
| CARD19 | 0.33 | 2.01E-04 | 0.26 | 3.95E-02 | -0.45 | 8.73E-05 |
| CASP10 | 0.27 | 1.36E-02 | 0.38 | 4.08E-02 | -0.41 | 4.78E-07 |
| CAVIN2 | 0.99 | 2.43E-11 | 1.19 | 1.29E-13 | -0.69 | 3.01E-02 |
| CBARP | 1.00 | 5.83E-02 | 1.32 | 7.36E-04 | -1.97 | 3.01E-03 |
| CBFA2T3 | 0.78 | 1.96E-04 | 0.96 | 3.66E-06 | -1.11 | 2.56E-04 |
| CBLC | 0.65 | 1.62E-04 | 0.65 | 7.37E-07 | -0.96 | 1.32E-29 |
| CBLN3 | 1.46 | 9.98E-06 | 1.59 | 8.65E-05 | -1.66 | 4.47E-05 |
| CBS | 1.23 | 1.73E-05 | 1.57 | 8.45E-06 | -1.18 | 6.78E-03 |
| CBSL | 4.23 | 6.42E-03 | 5.08 | 1.21E-04 | -3.46 | 9.11E-03 |
| CBX2 | 0.58 | 8.65E-03 | 0.86 | 3.63E-04 | -0.76 | 3.37E-05 |
| CCBE1 | 2.03 | 9.51E-03 | 3.42 | 2.29E-08 | -3.26 | 8.91E-05 |
| CCDC8 | 0.85 | 6.33E-02 | 1.77 | 5.97E-08 | -3.16 | 2.41E-05 |
| CCL2 | 5.38 | 4.14E-05 | 5.91 | 4.65E-07 | -2.91 | 1.68E-02 |
| CCND1 | 0.54 | 7.99E-02 | 1.04 | 2.39E-09 | -0.98 | 2.39E-02 |
| CCNE1 | 0.83 | 1.92E-03 | 1.11 | 1.16E-03 | -1.42 | 2.51E-09 |
| CD177 | 6.36 | 4.38E-38 | 5.84 | 1.50E-20 | -5.83 | 7.86E-03 |
| CD274 | 0.54 | 6.30E-02 | 0.83 | 3.53E-06 | -0.80 | 2.61E-02 |
| CD40 | 0.88 | 6.93E-04 | 1.00 | 2.77E-10 | -0.71 | 4.54E-06 |
| CD46 | 0.39 | 1.08E-02 | 0.43 | 1.49E-06 | -0.22 | 1.17E-02 |
| CD47 | 0.34 | 3.33E-04 | 0.45 | 2.68E-07 | -0.47 | 4.60E-03 |
| CDC25B | 0.77 | 1.84E-05 | 1.19 | 4.08E-02 | -1.58 | 7.81E-10 |
| CDC42EP1 | 0.54 | 3.58E-08 | 0.90 | 2.50E-09 | -1.35 | 1.35E-03 |
| CDCA7 | 0.79 | 2.27E-02 | 0.74 | 3.08E-02 | -1.72 | 9.00E-04 |
| CDCP1 | 0.29 | 7.51E-02 | 0.47 | 5.92E-07 | -0.63 | 6.74E-10 |
| CDH3 | 0.44 | 7.09E-03 | 0.74 | 7.49E-06 | -0.77 | 1.88E-02 |
| CDH4 | 1.37 | 2.00E-02 | 2.76 | 9.99E-15 | -1.91 | 7.42E-09 |
| CDH5 | 1.48 | 2.89E-03 | 1.62 | 1.57E-02 | -2.59 | 4.79E-04 |
| CDIP1 | 0.29 | 3.39E-02 | 0.31 | 3.28E-02 | -0.57 | 1.05E-02 |
| CDK16 | 0.19 | 8.88E-02 | 0.17 | 8.53E-02 | -0.22 | 1.65E-05 |
| CELF2 | 0.73 | 2.19E-02 | 1.25 | 7.74E-13 | -0.78 | 1.67E-04 |
| CELF4 | 1.35 | 4.68E-02 | 1.53 | 9.81E-02 | -1.16 | 1.84E-02 |
| CEP250 | 0.22 | 8.87E-02 | 0.28 | 7.08E-02 | -0.32 | 1.99E-06 |
| CERCAM | 1.34 | 2.79E-05 | 1.97 | 6.21E-16 | -2.40 | 1.11E-07 |
| CFL1 | 0.23 | 4.69E-02 | 0.37 | 1.18E-05 | -0.48 | 9.08E-03 |
| CFLAR | 0.28 | 3.79E-03 | 0.31 | 1.39E-03 | -0.52 | 4.01E-04 |
| CHAF1A | 0.34 | 3.65E-03 | 0.50 | 1.09E-02 | -0.67 | 1.46E-06 |
| CHI3L2 | 2.57 | 8.47E-03 | 4.45 | 4.21E-07 | -3.10 | 9.04E-05 |
| CHST11 | 0.75 | 4.19E-13 | 0.94 | 2.30E-13 | -0.76 | 5.05E-03 |
| CIB2 | 1.06 | 5.78E-03 | 1.35 | 3.49E-04 | -1.81 | 4.66E-29 |
| CIC | 0.22 | 6.23E-02 | 0.25 | 1.54E-02 | -0.33 | 3.32E-03 |
| CISH | 0.71 | 1.33E-03 | 1.17 | 1.48E-10 | -0.35 | 3.76E-02 |
| CKAP2 | 0.24 | 7.29E-02 | 0.49 | 1.18E-02 | -0.83 | 7.63E-22 |
| CKB | 0.37 | 5.83E-04 | 0.35 | 4.82E-03 | -0.75 | 4.23E-06 |

| | | | | | | |
|---|---|---|---|---|---|---|
| CLCN5 | 0.43 | 1.08E-02 | 0.48 | 1.99E-03 | -0.45 | 6.17E-03 |
| CLDN4 | 0.34 | 3.13E-02 | 0.35 | 1.38E-02 | -0.39 | 1.75E-04 |
| CLIC5 | 0.75 | 1.55E-04 | 0.92 | 5.79E-05 | -0.72 | 5.88E-03 |
| CMIP | 0.42 | 7.33E-03 | 0.54 | 8.30E-05 | -0.47 | 2.44E-03 |
| CMPK2 | 1.14 | 9.54E-04 | 1.39 | 3.41E-07 | -1.79 | 7.08E-04 |
| CNN2 | 0.53 | 1.39E-05 | 0.73 | 3.68E-11 | -0.77 | 3.85E-04 |
| CNTN1 | 1.53 | 2.21E-02 | 1.21 | 2.92E-06 | -1.60 | 4.90E-05 |
| CNTNAP2 | 0.67 | 7.44E-05 | 1.16 | 4.53E-09 | -1.43 | 1.59E-12 |
| COL17A1 | 0.47 | 3.19E-02 | 0.56 | 7.15E-03 | -0.70 | 8.09E-03 |
| COL6A1 | 1.91 | 3.39E-19 | 2.72 | 2.90E-24 | -2.16 | 3.13E-12 |
| COL8A2 | 1.22 | 1.07E-03 | 1.89 | 3.80E-07 | -1.28 | 1.93E-04 |
| COLGALT1 | 0.38 | 9.15E-02 | 0.54 | 5.62E-11 | -0.79 | 1.54E-02 |
| COTL1 | 0.45 | 8.89E-02 | 0.68 | 7.46E-12 | -1.17 | 5.81E-03 |
| CRYBB2P1 | 0.55 | 7.85E-02 | 0.60 | 5.87E-03 | -0.75 | 9.61E-08 |
| CRYBG2 | 0.67 | 6.25E-02 | 1.03 | 1.69E-07 | -1.54 | 3.08E-05 |
| CSF1 | 1.96 | 3.29E-04 | 1.70 | 4.46E-40 | -0.85 | 4.80E-03 |
| CSNK2A1 | 0.18 | 1.27E-02 | 0.21 | 1.36E-02 | -0.12 | 6.71E-03 |
| CSTB | 0.71 | 2.47E-02 | 0.80 | 1.78E-07 | -0.77 | 2.68E-02 |
| CTSE | 3.76 | 1.17E-16 | 5.97 | 1.38E-116 | -3.03 | 1.93E-05 |
| CXCL5 | 2.26 | 3.48E-18 | 4.04 | 1.74E-07 | -4.92 | 1.46E-08 |
| CYP1A1 | 3.85 | 6.19E-05 | 2.63 | 1.93E-08 | -1.81 | 2.04E-02 |
| CYP2E1 | 0.65 | 8.60E-02 | 1.07 | 1.98E-02 | -1.69 | 4.17E-08 |
| CYP4A22-AS1 | 1.80 | 3.12E-02 | 2.13 | 4.05E-02 | -1.45 | 4.18E-02 |
| CYTH3 | 0.42 | 4.46E-03 | 0.58 | 1.58E-06 | -0.86 | 1.44E-13 |
| DAPK1 | 0.98 | 9.09E-06 | 1.54 | 8.86E-17 | -1.03 | 7.45E-09 |
| DAPK3 | 0.23 | 4.73E-02 | 0.43 | 5.35E-06 | -0.70 | 3.40E-02 |
| DBNDD1 | 0.52 | 1.51E-02 | 0.64 | 8.85E-06 | -0.64 | 1.57E-03 |
| DCTN5 | 0.61 | 2.09E-16 | 0.60 | 6.42E-10 | -0.46 | 1.71E-12 |
| DDA1 | 0.26 | 6.80E-03 | 0.26 | 6.57E-02 | -0.33 | 9.53E-03 |
| DDIAS | 1.00 | 1.45E-02 | 0.96 | 1.34E-02 | -0.67 | 2.06E-02 |
| DEFB4A | 2.78 | 4.60E-05 | 6.94 | 2.43E-07 | -4.64 | 2.73E-07 |
| DENND3 | 0.51 | 5.00E-04 | 0.78 | 2.45E-06 | -0.99 | 8.79E-15 |
| DIP2C | 0.97 | 1.48E-05 | 1.59 | 1.05E-19 | -0.62 | 4.49E-02 |
| DLC1 | 2.07 | 2.14E-07 | 1.71 | 1.00E-05 | -1.52 | 8.24E-03 |
| DOCK1 | 0.37 | 6.16E-06 | 0.37 | 5.33E-03 | -0.37 | 1.05E-11 |
| DOCK7 | 0.42 | 3.45E-03 | 0.44 | 1.76E-05 | -0.44 | 3.27E-02 |
| DRAM1 | 0.53 | 2.30E-05 | 0.68 | 5.89E-11 | -0.62 | 2.40E-04 |
| DSC2 | 0.57 | 7.01E-02 | 1.37 | 6.30E-03 | -2.32 | 1.63E-05 |
| DST | 0.28 | 9.23E-02 | 0.42 | 5.03E-05 | -0.96 | 1.21E-07 |
| E2F3 | 0.35 | 3.36E-02 | 0.41 | 1.83E-02 | -0.66 | 2.82E-02 |
| EBI3 | 1.86 | 3.35E-03 | 2.88 | 1.67E-07 | -2.47 | 5.80E-04 |
| ECI2 | 0.54 | 8.42E-07 | 0.54 | 6.95E-04 | -0.58 | 7.60E-05 |
| EDA | 1.30 | 2.99E-03 | 1.49 | 4.11E-11 | -0.62 | 2.37E-03 |
| EDN1 | 0.83 | 7.44E-03 | 1.61 | 5.53E-08 | -2.20 | 4.23E-03 |
| EEA1 | 0.19 | 3.40E-02 | 0.19 | 8.39E-02 | -0.40 | 7.83E-03 |
| EFEMP2 | 0.44 | 9.47E-02 | 0.94 | 1.60E-08 | -1.11 | 7.63E-04 |
| EHBP1L1 | 0.23 | 6.19E-02 | 0.29 | 5.60E-02 | -0.35 | 3.81E-05 |
| EHD2 | 0.41 | 1.52E-03 | 0.46 | 4.31E-05 | -0.50 | 3.68E-08 |

| | | | | | | |
|---|---|---|---|---|---|---|
| EHD4 | 0.37 | 1.01E-11 | 0.40 | 5.21E-07 | -0.39 | 2.86E-07 |
| EIF2S2 | 0.17 | 3.43E-02 | 0.35 | 2.85E-04 | -0.19 | 1.65E-02 |
| EIF6 | 0.24 | 3.33E-02 | 0.33 | 3.32E-04 | -0.35 | 1.80E-06 |
| ELOVL6 | 0.55 | 7.07E-05 | 0.60 | 7.92E-08 | -0.82 | 8.59E-04 |
| ELOVL7 | 1.45 | 2.49E-24 | 1.27 | 2.94E-14 | -1.14 | 4.73E-07 |
| EMC1 | 0.38 | 6.66E-07 | 0.44 | 1.53E-06 | -0.55 | 6.46E-03 |
| EMP1 | 0.39 | 3.70E-02 | 0.68 | 1.30E-11 | -2.10 | 3.46E-05 |
| ENO1 | 0.34 | 5.64E-03 | 0.37 | 5.98E-06 | -0.24 | 3.73E-02 |
| EPB41L2 | 0.80 | 4.04E-02 | 0.94 | 9.78E-07 | -1.11 | 6.72E-10 |
| EPHB4 | 0.26 | 4.60E-03 | 0.32 | 9.50E-04 | -0.49 | 2.56E-05 |
| EPHX3 | 0.81 | 1.03E-03 | 1.32 | 7.55E-10 | -1.36 | 2.19E-04 |
| EPPK1 | 0.57 | 4.87E-03 | 0.91 | 9.80E-23 | -1.37 | 1.85E-05 |
| EPSTI1 | 1.01 | 1.18E-03 | 1.26 | 2.40E-06 | -2.03 | 2.56E-08 |
| ERFE | 1.98 | 3.13E-03 | 1.75 | 5.08E-02 | -2.00 | 1.45E-04 |
| ERRFI1 | 0.85 | 4.48E-07 | 1.11 | 8.65E-10 | -1.04 | 4.10E-02 |
| ERV3-1 | 1.32 | 1.59E-19 | 1.59 | 1.03E-25 | -0.97 | 6.94E-09 |
| ESS2 | 0.33 | 9.42E-03 | 0.35 | 1.26E-02 | -0.26 | 4.23E-02 |
| ETS1 | 0.30 | 1.48E-02 | 0.50 | 3.47E-05 | -0.85 | 8.82E-07 |
| ETV5 | 0.86 | 7.11E-02 | 1.91 | 1.32E-08 | -2.30 | 1.73E-05 |
| F11R | 0.17 | 6.79E-02 | 0.28 | 1.82E-03 | -0.28 | 1.43E-06 |
| F2R | 0.72 | 4.52E-02 | 0.87 | 1.99E-04 | -1.40 | 3.40E-10 |
| FAF2 | 0.16 | 8.49E-02 | 0.19 | 6.19E-02 | -0.12 | 2.92E-02 |
| FAH | 0.28 | 1.97E-02 | 0.32 | 1.90E-02 | -0.33 | 3.09E-02 |
| FAM105A | 1.99 | 8.62E-08 | 2.35 | 6.76E-19 | -1.84 | 3.41E-06 |
| FAM111B | 1.33 | 1.89E-06 | 1.84 | 4.24E-06 | -1.98 | 4.84E-15 |
| FAM129B | 0.26 | 9.36E-04 | 0.38 | 1.40E-04 | -0.39 | 4.39E-06 |
| FAM155B | 1.15 | 9.90E-02 | 1.46 | 1.21E-12 | -0.82 | 2.29E-03 |
| FAM198B | 1.13 | 9.58E-06 | 1.67 | 3.16E-09 | -1.62 | 5.78E-04 |
| FAM89A | 0.93 | 3.35E-03 | 0.95 | 2.33E-03 | -1.15 | 2.24E-04 |
| FARP2 | 0.33 | 4.76E-03 | 0.49 | 1.99E-04 | -0.60 | 2.28E-15 |
| FAT1 | 0.38 | 4.53E-02 | 0.57 | 1.06E-02 | -1.13 | 1.61E-02 |
| FBXO32 | 0.79 | 6.29E-06 | 0.89 | 1.63E-07 | -1.41 | 6.93E-06 |
| FCHO1 | 1.03 | 2.61E-02 | 1.09 | 1.26E-02 | -1.67 | 2.54E-05 |
| FGD3 | 0.64 | 2.53E-02 | 0.76 | 3.53E-02 | -1.23 | 8.33E-09 |
| FGD6 | 0.31 | 6.25E-02 | 0.59 | 3.76E-08 | -0.76 | 1.93E-02 |
| FGF11 | 0.36 | 1.35E-02 | 0.39 | 1.56E-04 | -0.74 | 2.10E-05 |
| FGF7P3 | 1.59 | 1.58E-05 | 1.73 | 8.62E-04 | -1.40 | 4.40E-02 |
| FHDC1 | 0.40 | 8.92E-03 | 0.54 | 4.34E-03 | -0.93 | 3.41E-04 |
| FKBP10 | 0.51 | 5.33E-02 | 0.69 | 2.39E-04 | -2.31 | 1.01E-05 |
| FLCN | 0.31 | 8.16E-04 | 0.37 | 1.17E-02 | -0.52 | 5.14E-07 |
| FLNA | 0.51 | 1.14E-02 | 1.01 | 3.70E-13 | -1.79 | 1.10E-02 |
| FLRT3 | 0.55 | 2.55E-07 | 0.84 | 1.68E-16 | -0.29 | 2.21E-02 |
| FMNL2 | 0.35 | 7.99E-02 | 0.26 | 6.68E-02 | -0.50 | 2.22E-07 |
| FN3KRP | 0.32 | 2.12E-02 | 0.30 | 4.79E-02 | -0.27 | 1.31E-03 |
| FOSL1 | 0.67 | 2.90E-07 | 0.92 | 7.31E-07 | -1.06 | 2.98E-02 |
| FOXE1 | 1.21 | 5.43E-06 | 1.52 | 1.22E-13 | -1.66 | 1.55E-18 |
| FOXL1 | 0.99 | 6.80E-06 | 0.91 | 1.16E-05 | -1.24 | 5.25E-06 |
| FP565260.1 | 0.43 | 8.34E-03 | 0.65 | 7.25E-04 | -0.49 | 4.84E-03 |
| FRMD5 | 0.66 | 5.34E-02 | 0.96 | 1.13E-03 | -1.34 | 8.15E-03 |

| | | | | | | |
|---|---|---|---|---|---|---|
| FSCN1 | 0.36 | 9.11E-02 | 0.37 | 1.14E-02 | -1.09 | 9.31E-04 |
| FSTL1 | 0.46 | 5.17E-02 | 0.83 | 1.44E-05 | -1.27 | 5.61E-05 |
| FTH1P11 | 0.41 | 4.90E-02 | 0.83 | 1.66E-03 | -0.68 | 9.66E-03 |
| FTH1P20 | 0.31 | 8.85E-02 | 0.89 | 5.74E-04 | -0.63 | 3.34E-02 |
| FTH1P3 | 0.63 | 2.43E-02 | 1.00 | 1.58E-03 | -0.64 | 1.89E-02 |
| FXYD5 | 0.55 | 1.32E-02 | 1.16 | 2.12E-08 | -2.01 | 1.64E-07 |
| FYN | 0.86 | 6.19E-05 | 1.16 | 1.70E-07 | -0.76 | 5.94E-03 |
| GAB2 | 0.37 | 4.30E-02 | 0.68 | 1.48E-05 | -0.59 | 4.12E-02 |
| GABRB3 | 3.29 | 9.45E-94 | 3.17 | 3.72E-18 | -2.37 | 1.73E-03 |
| GALNT14 | 0.62 | 8.16E-06 | 1.03 | 8.89E-09 | -0.88 | 1.99E-02 |
| GARS | 0.40 | 2.07E-05 | 0.71 | 3.95E-06 | -0.36 | 3.25E-02 |
| GATA6 | 0.38 | 1.61E-04 | 0.51 | 2.45E-05 | -0.32 | 4.01E-02 |
| GBP1 | 0.71 | 2.14E-10 | 0.82 | 3.43E-09 | -1.04 | 1.45E-02 |
| GBP2 | 0.62 | 5.24E-07 | 0.43 | 1.80E-03 | -0.30 | 4.58E-03 |
| GCNT2 | 0.30 | 6.52E-02 | 0.24 | 1.96E-02 | -0.21 | 1.55E-02 |
| GDE1 | 0.36 | 4.66E-02 | 0.27 | 7.28E-02 | -0.30 | 5.32E-03 |
| GDF15 | 1.01 | 5.24E-07 | 0.74 | 3.02E-06 | -0.93 | 1.36E-06 |
| GGH | 0.48 | 1.59E-07 | 0.30 | 7.32E-02 | -0.81 | 5.09E-11 |
| GM2A | 0.43 | 9.86E-02 | 0.44 | 3.53E-03 | -0.72 | 4.11E-10 |
| GNA15 | 0.26 | 3.52E-02 | 0.29 | 9.31E-04 | -0.35 | 4.27E-04 |
| GNG5 | 0.22 | 4.72E-02 | 0.25 | 7.97E-03 | -0.19 | 3.62E-02 |
| GPCPD1 | 0.35 | 1.79E-02 | 0.87 | 7.16E-05 | -0.50 | 1.42E-02 |
| GPLD1 | 0.64 | 3.80E-02 | 0.96 | 7.79E-04 | -0.37 | 4.48E-02 |
| GPR108 | 0.20 | 9.76E-02 | 0.28 | 9.46E-03 | -0.22 | 4.97E-02 |
| GPRC5A | 0.36 | 6.94E-02 | 0.48 | 1.18E-03 | -0.79 | 6.64E-03 |
| GRB10 | 0.40 | 2.88E-03 | 0.87 | 3.87E-16 | -1.01 | 4.12E-03 |
| GREB1L | 1.47 | 5.50E-03 | 1.93 | 5.33E-06 | -1.60 | 2.53E-03 |
| GSEC | 1.53 | 5.78E-02 | 1.77 | 7.54E-04 | -1.52 | 2.84E-03 |
| GSTM1 | 8.38 | 2.07E-05 | 8.94 | 1.57E-07 | -8.13 | 1.42E-05 |
| GSTM3 | 1.81 | 3.89E-04 | 2.40 | 6.08E-10 | -1.91 | 9.86E-10 |
| GSTM4 | 1.55 | 5.89E-09 | 1.73 | 1.43E-07 | -1.43 | 3.89E-02 |
| GTF2IP4 | 0.31 | 2.13E-02 | 0.50 | 2.20E-04 | -0.93 | 8.08E-06 |
| GTPBP2 | 0.18 | 7.19E-02 | 0.42 | 4.48E-05 | -0.56 | 7.08E-04 |
| GYS1 | 0.25 | 3.24E-02 | 0.30 | 1.20E-02 | -0.43 | 2.10E-02 |
| HAAO | 1.34 | 4.78E-02 | 1.63 | 1.15E-03 | -1.13 | 7.05E-03 |
| HAS3 | 1.11 | 1.11E-09 | 1.07 | 4.71E-09 | -0.95 | 1.24E-02 |
| HDHD3 | 0.48 | 2.89E-03 | 0.70 | 2.85E-04 | -0.69 | 3.06E-02 |
| HELZ2 | 0.27 | 2.14E-02 | 0.39 | 2.16E-02 | -0.70 | 4.01E-03 |
| HIC1 | 0.96 | 6.29E-02 | 1.23 | 1.87E-07 | -2.20 | 1.82E-02 |
| HJURP | 0.83 | 1.26E-02 | 0.84 | 2.68E-02 | -2.15 | 4.48E-07 |
| HKDC1 | 1.67 | 7.51E-24 | 2.87 | 5.85E-24 | -1.88 | 5.30E-05 |
| HLA-DOB | 1.32 | 7.11E-04 | 2.08 | 3.67E-08 | -1.26 | 1.53E-03 |
| HLA-DQB1 | 4.27 | 1.54E-06 | 4.97 | 5.04E-15 | -3.24 | 1.57E-03 |
| HLA-F | 0.88 | 4.56E-06 | 1.10 | 4.45E-16 | -0.45 | 4.41E-02 |
| HLA-G | 1.26 | 2.25E-04 | 1.79 | 2.17E-09 | -1.34 | 7.31E-07 |
| HLA-K | 1.09 | 4.63E-04 | 0.86 | 3.05E-02 | -1.01 | 3.43E-04 |
| HLA-L | 2.55 | 1.28E-29 | 2.15 | 8.21E-12 | -1.26 | 1.43E-03 |
| HLA-V | 0.88 | 3.50E-03 | 0.67 | 5.41E-02 | -1.15 | 6.74E-05 |
| HMGA1 | 0.19 | 3.60E-02 | 0.16 | 6.93E-02 | -0.77 | 1.77E-10 |

| | | | | | | |
|---|---|---|---|---|---|---|
| HOPX | 1.46 | 2.12E-08 | 2.75 | 1.20E-46 | -1.68 | 3.58E-02 |
| HORMAD1 | 5.42 | 2.55E-02 | 6.89 | 1.17E-02 | -6.21 | 5.09E-03 |
| HS6ST2 | 0.54 | 6.74E-04 | 0.70 | 3.51E-07 | -0.89 | 3.91E-11 |
| HSD17B1 | 0.67 | 8.36E-03 | 0.67 | 3.96E-02 | -0.68 | 2.48E-03 |
| HSD17B14 | 1.49 | 3.57E-06 | 1.45 | 3.05E-03 | -1.68 | 1.64E-04 |
| HSPG2 | 0.48 | 8.53E-03 | 0.72 | 4.16E-06 | -1.76 | 2.17E-04 |
| ICAM1 | 1.88 | 6.13E-27 | 1.86 | 4.95E-41 | -1.84 | 4.20E-04 |
| IDO1 | 1.12 | 7.00E-02 | 1.56 | 4.29E-11 | -1.86 | 1.33E-03 |
| IFFO2 | 0.30 | 3.13E-02 | 0.54 | 7.19E-05 | -1.10 | 3.97E-03 |
| IFI27 | 1.59 | 1.79E-02 | 2.74 | 4.62E-26 | -3.98 | 3.37E-23 |
| IFI27L2 | 0.50 | 1.90E-02 | 0.46 | 9.93E-03 | -0.85 | 7.73E-06 |
| IFI6 | 0.87 | 5.85E-04 | 1.38 | 1.13E-14 | -2.16 | 8.25E-12 |
| IFIT1 | 1.33 | 7.81E-02 | 0.88 | 2.43E-02 | -2.64 | 3.64E-06 |
| IFIT2 | 0.78 | 1.99E-16 | 0.49 | 1.48E-03 | -1.02 | 3.29E-02 |
| IFIT3 | 0.85 | 2.78E-06 | 0.79 | 1.70E-07 | -1.45 | 3.86E-04 |
| IL1A | 0.64 | 2.61E-03 | 2.15 | 8.84E-06 | -2.15 | 2.69E-03 |
| IL1B | 0.67 | 4.55E-02 | 2.36 | 3.80E-03 | -3.55 | 9.27E-04 |
| IL32 | 0.95 | 5.39E-07 | 1.37 | 4.40E-21 | -1.84 | 7.24E-04 |
| IRF9 | 0.41 | 6.72E-06 | 0.41 | 1.11E-04 | -0.69 | 1.00E-16 |
| ITGA4 | 3.12 | 1.62E-03 | 3.62 | 3.21E-05 | -3.25 | 1.43E-03 |
| ITGA5 | 0.66 | 1.46E-02 | 0.91 | 1.65E-08 | -1.22 | 8.10E-04 |
| ITPR2 | 0.70 | 1.29E-07 | 0.72 | 1.36E-09 | -0.96 | 2.13E-06 |
| JAG1 | 0.42 | 6.43E-02 | 0.74 | 1.28E-05 | -1.46 | 3.69E-02 |
| JAK3 | 0.92 | 4.12E-02 | 0.79 | 3.56E-02 | -0.99 | 1.03E-03 |
| KALRN | 0.62 | 7.34E-02 | 0.69 | 8.22E-02 | -0.94 | 4.84E-02 |
| KBTBD11 | 1.64 | 1.29E-03 | 1.73 | 2.94E-14 | -0.90 | 2.60E-02 |
| KCNIP3 | 3.59 | 1.22E-02 | 3.33 | 6.22E-08 | -3.99 | 3.01E-07 |
| KCNJ15 | 0.45 | 2.48E-02 | 0.65 | 2.01E-08 | -0.57 | 3.31E-04 |
| KCNN4 | 0.47 | 1.51E-02 | 0.69 | 2.96E-05 | -0.92 | 2.27E-06 |
| KCTD15 | 0.26 | 3.31E-02 | 0.39 | 8.09E-03 | -0.63 | 1.31E-03 |
| KIAA1549L | 1.55 | 2.50E-02 | 2.24 | 1.06E-12 | -3.29 | 2.33E-04 |
| KIF18B | 0.92 | 1.97E-02 | 0.97 | 6.85E-02 | -2.42 | 3.84E-07 |
| KIF9-AS1 | 0.87 | 6.35E-06 | 1.08 | 6.13E-06 | -0.68 | 1.09E-05 |
| KLHL5 | 0.21 | 8.15E-02 | 0.25 | 2.72E-02 | -0.42 | 2.55E-02 |
| KPNB1 | 0.19 | 2.04E-03 | 0.27 | 3.71E-03 | -0.29 | 5.25E-03 |
| KRT13 | 1.36 | 4.68E-02 | 1.04 | 5.16E-02 | -0.92 | 5.03E-03 |
| KRT8 | 0.22 | 6.77E-02 | 0.23 | 1.59E-02 | -0.51 | 2.81E-08 |
| L3MBTL3 | 0.69 | 7.07E-05 | 0.68 | 2.45E-05 | -0.88 | 7.60E-07 |
| LACTB | 0.26 | 4.37E-02 | 0.32 | 9.99E-03 | -0.46 | 3.53E-03 |
| LAMB1 | 0.44 | 7.23E-02 | 0.64 | 5.45E-05 | -1.47 | 2.48E-06 |
| LAMC1 | 0.33 | 3.13E-02 | 0.37 | 7.54E-04 | -0.84 | 6.77E-05 |
| LAMP3 | 0.88 | 4.98E-04 | 1.32 | 1.59E-07 | -1.46 | 1.08E-07 |
| LARP1 | 0.28 | 4.01E-02 | 0.25 | 9.23E-03 | -0.20 | 5.78E-04 |
| LCP1 | 1.90 | 1.34E-11 | 2.61 | 2.94E-14 | -2.91 | 3.56E-06 |
| LDHB | 0.27 | 1.39E-02 | 0.16 | 8.21E-02 | -0.36 | 1.70E-03 |
| LEMD1 | 1.13 | 4.12E-02 | 1.41 | 3.14E-02 | -1.76 | 7.79E-04 |
| LGALSL | 0.35 | 1.90E-03 | 0.66 | 1.19E-05 | -0.47 | 8.78E-03 |
| LIF | 0.92 | 1.78E-04 | 0.72 | 1.33E-04 | -3.15 | 5.04E-03 |
| LIMCH1 | 1.54 | 3.48E-09 | 2.11 | 5.39E-37 | -0.97 | 6.07E-04 |

| | | | | | | |
|---|---|---|---|---|---|---|
| LINC00960 | 1.80 | 9.98E-02 | 2.03 | 1.04E-02 | -1.67 | 9.58E-04 |
| LINC00982 | 1.26 | 3.29E-02 | 1.35 | 5.44E-03 | -0.84 | 3.58E-02 |
| LINC01913 | 1.70 | 8.50E-03 | 1.92 | 8.76E-03 | -1.78 | 3.39E-02 |
| LINC02574 | 1.14 | 1.11E-04 | 1.45 | 3.02E-09 | -2.25 | 6.99E-14 |
| LMNB2 | 0.27 | 3.55E-02 | 0.27 | 4.18E-03 | -0.63 | 2.47E-03 |
| LOXL2 | 1.04 | 1.45E-07 | 1.12 | 2.85E-09 | -1.87 | 2.52E-02 |
| LPIN1 | 0.45 | 1.33E-02 | 0.55 | 4.25E-04 | -0.31 | 6.96E-03 |
| LRRC3 | 0.99 | 8.10E-02 | 1.53 | 6.67E-04 | -1.84 | 3.85E-02 |
| LTA4H | 1.24 | 4.88E-53 | 1.38 | 2.05E-42 | -1.00 | 7.80E-04 |
| LTB | 2.22 | 2.23E-07 | 2.53 | 7.14E-09 | -2.18 | 6.31E-04 |
| LY6K | 1.20 | 6.48E-03 | 1.52 | 5.93E-04 | -1.25 | 3.09E-02 |
| MAP2K2 | 0.22 | 6.34E-02 | 0.25 | 2.82E-03 | -0.80 | 3.37E-06 |
| MAP4 | 0.29 | 1.14E-02 | 0.55 | 6.14E-07 | -0.79 | 1.77E-02 |
| MAP4K4 | 0.30 | 8.58E-02 | 0.37 | 1.41E-03 | -0.69 | 2.74E-03 |
| MAPK3 | 0.38 | 6.43E-04 | 0.46 | 1.18E-05 | -0.34 | 9.57E-03 |
| MARCKS | 0.33 | 3.13E-02 | 0.44 | 1.76E-03 | -0.75 | 2.56E-02 |
| MBNL1 | 0.23 | 1.99E-02 | 0.33 | 2.23E-03 | -0.37 | 5.59E-08 |
| MELTF | 1.22 | 1.56E-03 | 1.82 | 2.60E-25 | -1.51 | 1.18E-04 |
| MET | 0.47 | 3.21E-02 | 0.74 | 6.24E-10 | -0.48 | 2.62E-09 |
| MFSD3 | 0.46 | 2.81E-06 | 0.57 | 3.10E-07 | -0.31 | 4.42E-02 |
| MICAL2 | 0.76 | 5.46E-14 | 1.12 | 6.50E-44 | -0.40 | 2.56E-02 |
| MILR1 | 1.95 | 6.86E-04 | 2.16 | 1.10E-13 | -1.72 | 8.93E-05 |
| MIR1307 | 4.24 | 6.78E-03 | 4.05 | 2.14E-02 | -3.57 | 5.71E-03 |
| MKI67 | 0.80 | 6.24E-05 | 0.52 | 5.59E-02 | -2.32 | 4.38E-07 |
| MKNK2 | 0.55 | 2.62E-04 | 0.40 | 7.31E-03 | -0.21 | 3.58E-04 |
| MLKL | 0.71 | 9.08E-05 | 0.72 | 2.25E-04 | -0.77 | 6.77E-08 |
| MMD | 0.58 | 4.86E-06 | 0.84 | 3.96E-09 | -0.70 | 8.77E-03 |
| MMP1 | 1.67 | 1.22E-11 | 3.43 | 1.89E-05 | -1.35 | 1.22E-04 |
| MRAS | 0.86 | 8.32E-07 | 1.44 | 5.10E-22 | -0.91 | 1.56E-02 |
| MSN | 0.27 | 4.69E-02 | 0.65 | 8.91E-07 | -1.16 | 2.10E-03 |
| MSNP1 | 0.65 | 4.66E-02 | 0.72 | 3.59E-02 | -1.02 | 1.86E-02 |
| MSRB2 | 0.24 | 2.20E-02 | 0.40 | 6.72E-04 | -0.18 | 1.67E-02 |
| MTCL1 | 0.41 | 3.02E-02 | 0.73 | 3.50E-05 | -1.27 | 3.58E-04 |
| MTHFD1L | 0.63 | 1.98E-06 | 0.90 | 2.69E-09 | -1.04 | 1.18E-02 |
| MTND3P25 | 5.10 | 5.74E-03 | 5.62 | 9.78E-02 | -4.71 | 2.00E-02 |
| MX1 | 0.75 | 2.53E-03 | 0.78 | 2.03E-07 | -1.44 | 3.70E-06 |
| MYADM | 0.55 | 7.06E-05 | 0.84 | 1.66E-11 | -0.97 | 1.68E-03 |
| MYH9 | 0.27 | 1.07E-02 | 0.55 | 1.20E-06 | -1.05 | 1.58E-02 |
| MYO1C | 0.20 | 1.57E-02 | 0.31 | 2.90E-04 | -0.31 | 3.92E-02 |
| NABP1 | 0.40 | 5.38E-02 | 0.98 | 9.78E-07 | -2.18 | 1.10E-05 |
| NACC1 | 0.24 | 3.44E-02 | 0.20 | 3.71E-02 | -0.17 | 9.89E-03 |
| NBPF10 | 0.52 | 1.02E-03 | 0.50 | 1.24E-02 | -0.42 | 3.81E-03 |
| NBPF14 | 0.70 | 7.42E-03 | 0.74 | 1.33E-04 | -0.42 | 8.13E-03 |
| NCAM2 | 2.34 | 1.21E-02 | 3.72 | 4.35E-05 | -2.38 | 2.85E-02 |
| NCAPG | 0.92 | 2.93E-02 | 0.82 | 1.66E-02 | -2.08 | 1.05E-06 |
| NDC1 | 0.24 | 3.78E-02 | 0.25 | 9.25E-02 | -0.48 | 1.13E-04 |
| NDN | 1.04 | 9.94E-04 | 1.63 | 7.93E-08 | -1.62 | 4.05E-16 |
| NEDD9 | 1.04 | 2.51E-10 | 1.69 | 1.47E-19 | -1.15 | 1.85E-02 |
| NIPSNAP1 | 0.28 | 6.97E-03 | 0.35 | 5.88E-04 | -0.39 | 6.41E-05 |

| | | | | | | |
|---|---|---|---|---|---|---|
| NKX2-1 | 1.47 | 4.13E-05 | 2.21 | 6.93E-24 | -1.26 | 9.29E-03 |
| NLRC5 | 0.62 | 6.94E-04 | 0.75 | 6.27E-04 | -0.73 | 5.62E-05 |
| NMD3 | 0.27 | 3.14E-03 | 0.30 | 3.23E-03 | -0.22 | 3.79E-03 |
| NME4 | 0.35 | 2.12E-02 | 0.50 | 3.37E-05 | -0.40 | 1.64E-02 |
| NMT2 | 0.39 | 7.93E-02 | 0.47 | 6.43E-02 | -1.03 | 1.86E-03 |
| NOP14-AS1 | 0.21 | 6.29E-02 | 0.53 | 8.24E-06 | -0.91 | 1.39E-02 |
| NOTCH2NL | 0.77 | 1.45E-04 | 0.60 | 6.82E-03 | -0.41 | 3.01E-03 |
| NOTCH3 | 0.38 | 5.55E-02 | 0.49 | 4.75E-03 | -0.94 | 1.14E-02 |
| NPC1 | 0.47 | 4.39E-07 | 0.72 | 1.32E-11 | -0.84 | 2.31E-05 |
| NPFFR2 | 3.56 | 2.04E-04 | 3.57 | 1.27E-03 | -4.10 | 2.46E-03 |
| NREP | 0.37 | 8.52E-02 | 0.68 | 2.62E-07 | -0.67 | 3.64E-05 |
| NRG1 | 0.59 | 1.44E-03 | 1.25 | 1.53E-08 | -0.88 | 4.77E-02 |
| NRIP1 | 0.50 | 5.71E-04 | 0.57 | 1.67E-07 | -0.78 | 3.18E-03 |
| NT5E | 0.73 | 6.41E-03 | 1.90 | 2.58E-53 | -2.11 | 3.50E-05 |
| NUDT2 | 0.51 | 3.57E-02 | 0.63 | 2.54E-04 | -0.57 | 4.37E-05 |
| NUP205 | 0.23 | 7.13E-02 | 0.27 | 4.14E-03 | -0.46 | 1.90E-02 |
| OAS1 | 0.34 | 1.13E-03 | 0.34 | 9.22E-02 | -0.65 | 4.12E-02 |
| OAS3 | 0.45 | 2.90E-03 | 0.55 | 1.08E-06 | -1.34 | 8.46E-08 |
| OASL | 1.69 | 1.12E-13 | 1.04 | 3.05E-02 | -1.19 | 1.39E-02 |
| OCLN | 0.32 | 4.10E-03 | 0.42 | 3.61E-04 | -0.77 | 2.73E-03 |
| OPA1 | 0.28 | 1.30E-03 | 0.33 | 8.28E-04 | -0.23 | 4.14E-03 |
| OSGIN2 | 0.29 | 2.15E-02 | 0.43 | 9.56E-04 | -0.24 | 6.90E-03 |
| OSMR | 0.49 | 8.47E-04 | 0.76 | 7.86E-16 | -0.39 | 5.54E-04 |
| OTULIN | 0.28 | 9.32E-03 | 0.28 | 3.38E-03 | -0.33 | 1.89E-07 |
| P2RY2 | 0.32 | 5.74E-02 | 0.51 | 3.35E-05 | -0.57 | 1.24E-02 |
| PADI3 | 1.18 | 2.33E-03 | 1.32 | 1.40E-04 | -1.32 | 1.09E-03 |
| PAK1 | 0.39 | 1.20E-05 | 0.54 | 7.69E-10 | -0.36 | 5.55E-03 |
| PALLD | 0.35 | 1.17E-02 | 0.65 | 1.59E-07 | -0.67 | 2.59E-02 |
| PAQR7 | 0.36 | 4.69E-02 | 0.79 | 1.75E-08 | -0.86 | 9.55E-08 |
| PARP14 | 0.58 | 1.20E-05 | 0.58 | 3.08E-12 | -0.51 | 3.79E-03 |
| PARP9 | 0.32 | 3.10E-02 | 0.45 | 5.98E-04 | -0.36 | 8.38E-03 |
| PATL1 | 0.45 | 8.40E-04 | 0.36 | 1.04E-04 | -0.30 | 1.34E-09 |
| PBX3 | 0.34 | 2.43E-02 | 0.35 | 1.79E-02 | -0.64 | 6.88E-08 |
| PCSK7 | 0.26 | 8.16E-02 | 0.40 | 4.83E-04 | -0.37 | 9.73E-07 |
| PCSK9 | 1.58 | 4.70E-08 | 1.65 | 1.70E-03 | -2.21 | 1.15E-11 |
| PDCD5 | 0.40 | 1.89E-05 | 0.45 | 3.55E-06 | -0.36 | 2.10E-02 |
| PDE4C | 2.13 | 1.40E-05 | 2.01 | 2.36E-04 | -2.56 | 6.30E-04 |
| PEG3 | 1.56 | 1.68E-02 | 2.44 | 8.05E-04 | -1.78 | 1.42E-03 |
| PER1 | 0.54 | 1.90E-05 | 0.44 | 6.30E-03 | -0.56 | 1.78E-02 |
| PEX14 | 0.20 | 7.35E-02 | 0.22 | 9.64E-02 | -0.20 | 5.63E-03 |
| PFKFB3 | 0.42 | 2.13E-03 | 0.75 | 7.51E-08 | -0.35 | 1.32E-02 |
| PFKFB4 | 0.64 | 5.83E-03 | 0.62 | 8.57E-06 | -0.72 | 3.45E-02 |
| PFKP | 0.44 | 9.05E-04 | 0.27 | 7.73E-02 | -0.32 | 4.71E-02 |
| PGGHG | 0.77 | 1.05E-02 | 1.25 | 7.33E-03 | -0.75 | 2.41E-02 |
| PHF19 | 0.55 | 1.26E-02 | 0.50 | 2.23E-02 | -1.08 | 1.47E-07 |
| PHF20 | 0.25 | 6.78E-02 | 0.33 | 1.89E-03 | -0.24 | 2.30E-03 |
| PICALM | 0.15 | 5.15E-02 | 0.19 | 3.71E-02 | -0.22 | 1.58E-03 |
| PIP5K1A | 0.25 | 4.77E-03 | 0.23 | 3.12E-02 | -0.16 | 1.93E-02 |
| PKD1P5 | 2.04 | 7.26E-29 | 1.84 | 2.31E-18 | -1.41 | 1.28E-03 |

| | | | | | | |
|---|---|---|---|---|---|---|
| PKP2 | 0.22 | 3.13E-02 | 0.23 | 5.20E-02 | -0.31 | 9.29E-05 |
| PLAGL1 | 0.41 | 1.88E-02 | 0.36 | 5.62E-02 | -0.54 | 2.24E-04 |
| PLAU | 0.71 | 5.71E-03 | 0.96 | 6.69E-09 | -2.15 | 1.06E-03 |
| PLD2 | 1.03 | 1.39E-18 | 1.00 | 2.24E-27 | -0.82 | 2.14E-05 |
| PLEC | 0.24 | 4.10E-02 | 0.53 | 1.31E-09 | -0.60 | 1.23E-03 |
| PLIN2 | 0.60 | 2.50E-03 | 0.49 | 2.65E-06 | -0.45 | 7.51E-03 |
| PLIN3 | 0.19 | 5.19E-02 | 0.26 | 2.53E-03 | -0.35 | 2.66E-04 |
| PLXND1 | 1.61 | 5.81E-19 | 1.98 | 4.41E-36 | -1.02 | 9.57E-04 |
| PML | 0.32 | 3.70E-03 | 0.53 | 1.24E-04 | -0.69 | 1.43E-03 |
| PNLDC1 | 3.80 | 8.53E-03 | 4.25 | 2.60E-04 | -3.70 | 6.30E-03 |
| POP1 | 0.58 | 1.45E-04 | 0.79 | 3.72E-03 | -1.02 | 6.51E-08 |
| POTEE | 0.72 | 1.29E-04 | 0.77 | 1.92E-06 | -0.63 | 2.48E-02 |
| PPA1 | 0.33 | 8.68E-03 | 0.45 | 4.47E-06 | -0.15 | 1.13E-02 |
| PRC1 | 0.56 | 9.32E-03 | 0.45 | 8.55E-02 | -1.68 | 1.10E-11 |
| PRELID1 | 0.23 | 5.15E-03 | 0.26 | 1.89E-02 | -0.27 | 1.53E-02 |
| PRKAR1B | 0.45 | 1.29E-02 | 0.58 | 6.30E-03 | -0.70 | 3.85E-03 |
| PRKCH | 0.36 | 2.90E-03 | 0.34 | 1.33E-03 | -0.37 | 2.07E-05 |
| PROM2 | 0.41 | 2.37E-04 | 0.46 | 3.27E-04 | -0.29 | 4.19E-02 |
| PROSER2 | 0.70 | 5.82E-07 | 0.69 | 1.18E-05 | -0.47 | 5.49E-08 |
| PRR11 | 0.87 | 3.31E-03 | 0.70 | 4.73E-03 | -2.23 | 6.11E-11 |
| PRSS1 | 2.15 | 7.04E-02 | 5.04 | 4.37E-10 | -3.57 | 5.82E-04 |
| PRSS2 | 2.19 | 6.26E-02 | 4.58 | 3.92E-15 | -3.40 | 2.23E-05 |
| PRSS21 | 2.61 | 4.36E-09 | 2.27 | 1.26E-09 | -1.70 | 7.69E-03 |
| PRSS22 | 0.56 | 1.54E-13 | 0.74 | 1.18E-04 | -0.33 | 4.21E-03 |
| PSAT1 | 1.20 | 2.38E-04 | 1.89 | 1.87E-04 | -0.50 | 2.87E-02 |
| PSCA | 2.19 | 3.12E-03 | 2.72 | 8.42E-03 | -2.74 | 3.82E-02 |
| PTGES2 | 0.19 | 4.35E-02 | 0.20 | 7.48E-02 | -0.26 | 1.02E-02 |
| PTPN20 | 1.89 | 2.25E-10 | 1.79 | 2.01E-06 | -1.77 | 7.28E-03 |
| PTPRF | 0.25 | 3.39E-02 | 0.28 | 2.72E-02 | -0.57 | 7.92E-03 |
| PVR | 0.36 | 1.04E-02 | 0.91 | 5.34E-13 | -0.89 | 5.47E-03 |
| QPCT | 0.43 | 8.61E-02 | 0.80 | 5.99E-04 | -1.41 | 3.48E-04 |
| RAB11FIP1 | 0.33 | 2.94E-02 | 0.56 | 5.79E-06 | -1.25 | 1.51E-03 |
| RAB31 | 0.52 | 1.15E-06 | 0.55 | 3.26E-07 | -0.26 | 3.18E-02 |
| RAB32 | 0.39 | 7.28E-04 | 0.67 | 1.91E-08 | -0.77 | 1.04E-03 |
| RAB6B | 1.90 | 3.22E-10 | 1.99 | 3.42E-06 | -2.04 | 4.43E-03 |
| RAC2 | 0.52 | 1.59E-02 | 0.93 | 1.96E-08 | -1.29 | 9.42E-04 |
| RAP1GAP2 | 0.65 | 9.02E-04 | 1.27 | 3.11E-25 | -0.91 | 9.66E-05 |
| RASGEF1A | 1.17 | 4.47E-04 | 1.48 | 2.69E-04 | -1.96 | 4.42E-04 |
| RASGRP3 | 1.16 | 1.82E-03 | 1.45 | 1.50E-03 | -1.46 | 4.70E-04 |
| RASSF3 | 0.40 | 1.04E-03 | 0.48 | 9.83E-05 | -0.75 | 4.17E-08 |
| RBMS2 | 0.26 | 3.00E-03 | 0.28 | 1.85E-03 | -0.34 | 7.02E-06 |
| RCAN1 | 0.24 | 7.17E-02 | 0.64 | 3.43E-09 | -0.58 | 2.45E-02 |
| RCBTB1 | 0.28 | 7.45E-02 | 0.43 | 3.97E-03 | -0.45 | 7.00E-03 |
| RCOR1 | 0.24 | 2.96E-02 | 0.24 | 4.85E-03 | -0.31 | 1.80E-12 |
| REC8 | 1.21 | 1.37E-43 | 1.61 | 2.37E-25 | -2.20 | 2.03E-31 |
| RELL1 | 0.80 | 1.13E-07 | 0.88 | 2.46E-08 | -0.54 | 4.12E-02 |
| RELT | 0.55 | 2.68E-02 | 0.75 | 2.09E-03 | -1.05 | 9.09E-03 |
| RENBP | 2.59 | 1.99E-05 | 3.37 | 2.40E-06 | -2.78 | 2.39E-09 |
| RFX7 | 0.48 | 6.84E-07 | 0.42 | 1.20E-03 | -0.72 | 3.72E-21 |

| | | | | | | |
|---|---|---|---|---|---|---|
| RGS10 | 0.42 | 1.89E-02 | 0.45 | 4.95E-02 | -1.38 | 8.99E-05 |
| RGS20 | 0.70 | 9.36E-04 | 0.80 | 1.81E-03 | -1.84 | 4.88E-06 |
| RHBDF2 | 0.24 | 2.23E-02 | 0.37 | 1.05E-02 | -0.92 | 1.83E-02 |
| RHCG | 0.84 | 1.13E-04 | 3.34 | 3.94E-03 | -3.91 | 2.28E-08 |
| RHOBTB3 | 0.36 | 2.75E-03 | 0.59 | 6.80E-05 | -0.35 | 6.87E-03 |
| RHOF | 1.66 | 1.42E-47 | 2.19 | 5.52E-72 | -2.13 | 3.22E-22 |
| RIPOR1 | 0.31 | 1.87E-02 | 0.47 | 6.48E-05 | -0.57 | 3.16E-03 |
| RND3 | 0.28 | 2.39E-02 | 0.33 | 8.95E-05 | -0.63 | 3.04E-02 |
| RNF144A | 1.05 | 3.10E-03 | 1.52 | 1.13E-05 | -1.05 | 5.70E-07 |
| RNF216P1 | 0.52 | 1.27E-04 | 0.68 | 3.14E-05 | -0.40 | 3.14E-04 |
| ROBO3 | 0.92 | 2.84E-03 | 1.17 | 5.33E-05 | -1.38 | 1.74E-11 |
| RPL10P9 | 0.95 | 3.34E-02 | 0.83 | 8.58E-03 | -0.83 | 3.18E-02 |
| RPL29 | 0.26 | 9.87E-02 | 0.26 | 2.88E-03 | -0.37 | 2.99E-04 |
| RPSAP58 | 0.71 | 1.07E-09 | 0.40 | 1.70E-03 | -0.35 | 3.10E-02 |
| RRM2 | 0.62 | 7.21E-02 | 0.82 | 6.57E-03 | -1.70 | 5.08E-04 |
| RRP7A | 0.30 | 3.00E-03 | 0.35 | 1.30E-04 | -0.25 | 1.10E-03 |
| RSAD2 | 1.96 | 1.08E-04 | 2.33 | 3.22E-09 | -2.96 | 7.79E-10 |
| RTL8C | 0.28 | 3.69E-03 | 0.36 | 3.23E-05 | -0.48 | 3.53E-02 |
| S1PR5 | 0.87 | 6.15E-09 | 1.00 | 2.97E-09 | -0.83 | 1.16E-08 |
| SALL4 | 1.82 | 4.79E-03 | 1.90 | 2.96E-05 | -2.30 | 4.50E-05 |
| SAMD4A | 0.45 | 1.50E-04 | 0.52 | 1.22E-02 | -0.81 | 4.08E-02 |
| SARS | 0.27 | 3.36E-03 | 0.33 | 4.04E-03 | -0.26 | 1.05E-02 |
| SAT1 | 0.19 | 7.06E-03 | 0.29 | 3.12E-03 | -0.18 | 2.21E-04 |
| SCD | 0.67 | 4.30E-03 | 0.92 | 3.96E-02 | -0.89 | 9.61E-08 |
| SCRN2 | 0.29 | 2.12E-02 | 0.51 | 1.33E-04 | -0.46 | 3.90E-09 |
| SDC1 | 0.24 | 8.40E-02 | 0.52 | 2.57E-04 | -0.47 | 2.22E-09 |
| SEMA3E | 0.94 | 1.63E-06 | 0.73 | 1.01E-02 | -0.54 | 2.02E-02 |
| SERPINB7 | 0.57 | 6.58E-03 | 2.38 | 2.36E-03 | -0.91 | 2.14E-03 |
| SERPINB9 | 1.03 | 1.02E-10 | 1.17 | 3.99E-15 | -2.25 | 3.04E-07 |
| SERPINH1 | 0.36 | 7.49E-07 | 0.64 | 1.71E-11 | -0.56 | 2.76E-03 |
| SESN2 | 0.32 | 2.50E-03 | 0.52 | 7.03E-05 | -0.37 | 7.98E-03 |
| SFN | 0.31 | 3.86E-02 | 0.59 | 3.46E-06 | -0.91 | 8.21E-05 |
| SGTB | 0.44 | 9.62E-02 | 0.60 | 1.10E-02 | -0.65 | 2.29E-02 |
| SH2B3 | 0.60 | 2.69E-03 | 0.43 | 6.26E-03 | -0.48 | 2.59E-04 |
| SH3BP2 | 0.64 | 2.41E-03 | 0.56 | 1.82E-06 | -0.52 | 4.16E-05 |
| SH3TC2 | 0.40 | 8.10E-02 | 0.52 | 3.02E-04 | -1.47 | 6.05E-03 |
| SHANK3 | 0.55 | 1.32E-02 | 0.79 | 1.97E-04 | -0.69 | 2.40E-03 |
| SHC1 | 0.28 | 1.26E-02 | 0.35 | 4.39E-03 | -0.29 | 1.35E-02 |
| SIPA1 | 0.55 | 8.63E-05 | 0.62 | 4.10E-05 | -0.43 | 4.62E-03 |
| SIRPB2 | 1.39 | 1.38E-02 | 1.19 | 5.91E-02 | -1.06 | 7.91E-03 |
| SLC12A5 | 1.65 | 9.02E-02 | 2.56 | 1.43E-02 | -1.36 | 2.26E-02 |
| SLC15A4 | 0.26 | 1.80E-02 | 0.45 | 3.90E-05 | -0.37 | 3.17E-02 |
| SLC16A1 | 0.71 | 5.98E-06 | 0.73 | 3.37E-05 | -0.54 | 6.85E-03 |
| SLC16A12 | 0.63 | 8.54E-02 | 0.86 | 4.62E-02 | -1.27 | 2.80E-02 |
| SLC26A9 | 1.06 | 4.71E-02 | 2.72 | 8.13E-06 | -2.09 | 3.32E-06 |
| SLC2A14 | 2.66 | 8.10E-03 | 2.23 | 5.49E-02 | -2.33 | 5.61E-03 |
| SLC2A5 | 1.20 | 4.36E-02 | 1.93 | 7.31E-04 | -2.99 | 6.33E-03 |
| SLC2A6 | 1.17 | 1.12E-13 | 1.32 | 1.47E-19 | -2.15 | 2.05E-03 |
| SLC35F2 | 0.74 | 2.91E-12 | 0.91 | 3.68E-14 | -1.23 | 2.54E-07 |

| | | | | | | |
|---|---|---|---|---|---|---|
| SLC44A1 | 0.26 | 1.43E-03 | 0.32 | 1.03E-03 | -0.34 | 1.46E-05 |
| SLC44A3-AS1 | 0.35 | 7.33E-02 | 0.67 | 6.62E-04 | -0.66 | 4.18E-07 |
| SLC6A11 | 1.19 | 6.36E-02 | 2.09 | 2.11E-06 | -1.42 | 5.14E-07 |
| SLC9A1 | 0.30 | 8.58E-02 | 0.48 | 5.27E-06 | -0.45 | 2.47E-04 |
| SLIT2 | 2.52 | 1.74E-02 | 1.98 | 4.46E-03 | -2.81 | 2.63E-05 |
| SMCO2 | 2.11 | 8.10E-02 | 2.95 | 6.64E-03 | -2.81 | 2.63E-03 |
| SMG6 | 0.15 | 8.17E-02 | 0.21 | 5.08E-02 | -0.34 | 4.64E-02 |
| SMIM10L2A | 1.15 | 5.31E-10 | 1.35 | 7.18E-11 | -1.48 | 3.65E-11 |
| SNCG | 0.86 | 1.27E-02 | 0.81 | 3.22E-02 | -2.41 | 5.77E-13 |
| SNHG17 | 0.75 | 9.16E-02 | 0.65 | 6.43E-02 | -0.45 | 5.36E-03 |
| SNHG5 | 1.95 | 8.89E-12 | 1.95 | 4.21E-24 | -1.77 | 1.39E-03 |
| SNHG7 | 0.77 | 2.85E-05 | 0.69 | 8.31E-09 | -0.62 | 3.83E-03 |
| SNHG8 | 0.42 | 3.78E-02 | 0.31 | 1.46E-02 | -0.32 | 6.96E-03 |
| SNRPF | 0.23 | 7.35E-02 | 0.26 | 2.92E-02 | -0.31 | 2.90E-03 |
| SNRPN | 0.23 | 2.83E-03 | 0.39 | 4.24E-06 | -0.26 | 7.37E-03 |
| SNURF | 0.22 | 4.75E-02 | 0.38 | 3.47E-05 | -0.26 | 1.61E-02 |
| SOHLH2 | 2.42 | 1.57E-04 | 3.12 | 2.82E-07 | -2.11 | 3.68E-02 |
| SPATA5L1 | 0.43 | 1.24E-02 | 0.59 | 4.02E-05 | -0.50 | 3.79E-05 |
| SPC24 | 0.93 | 1.63E-02 | 0.89 | 7.85E-02 | -1.90 | 1.45E-08 |
| SPIRE1 | 0.49 | 2.70E-10 | 0.23 | 1.35E-02 | -0.29 | 3.18E-02 |
| SPRED3 | 0.70 | 1.28E-02 | 0.77 | 1.06E-02 | -0.94 | 1.35E-03 |
| SPRR2A | 1.38 | 1.10E-03 | 5.19 | 4.88E-04 | -4.75 | 1.21E-19 |
| SPRR2D | 1.49 | 3.92E-05 | 3.92 | 5.60E-04 | -4.08 | 1.70E-14 |
| SPRR2F | 3.18 | 1.32E-03 | 7.05 | 6.39E-05 | -4.72 | 9.10E-08 |
| SRC | 0.29 | 2.99E-02 | 0.53 | 1.99E-07 | -0.69 | 1.15E-06 |
| SRPX2 | 0.93 | 1.00E-10 | 0.94 | 4.60E-13 | -1.08 | 1.75E-08 |
| SSH1 | 0.43 | 4.70E-03 | 0.31 | 1.48E-02 | -0.37 | 1.97E-02 |
| ST3GAL4 | 1.17 | 3.04E-04 | 1.00 | 7.18E-11 | -0.43 | 2.92E-02 |
| STARD4 | 0.34 | 1.26E-02 | 0.38 | 1.93E-02 | -0.52 | 1.08E-10 |
| STC2 | 1.46 | 3.61E-05 | 2.14 | 5.29E-05 | -1.61 | 7.71E-03 |
| STMN1 | 0.56 | 2.71E-02 | 0.86 | 3.15E-14 | -1.84 | 8.72E-08 |
| STON1 | 1.24 | 4.79E-02 | 1.63 | 1.80E-03 | -2.25 | 2.54E-05 |
| STRIP2 | 1.22 | 7.33E-03 | 1.41 | 6.13E-06 | -1.02 | 2.91E-03 |
| SUSD2 | 1.06 | 2.46E-03 | 1.97 | 1.34E-13 | -2.39 | 2.22E-05 |
| SVIL | 0.57 | 3.04E-03 | 0.92 | 2.05E-10 | -1.37 | 5.50E-03 |
| SVILP1 | 0.95 | 7.33E-03 | 0.86 | 8.62E-02 | -1.40 | 2.62E-02 |
| SYCP2L | 3.58 | 3.00E-02 | 3.78 | 9.72E-02 | -2.86 | 3.40E-02 |
| SYT16 | 1.07 | 1.73E-05 | 0.97 | 2.50E-03 | -1.37 | 3.03E-07 |
| TAP1 | 0.39 | 1.17E-04 | 0.50 | 1.20E-08 | -0.61 | 1.12E-05 |
| TAP2 | 0.27 | 1.00E-01 | 0.40 | 3.25E-05 | -0.30 | 1.25E-02 |
| TCF19 | 0.46 | 2.22E-02 | 0.49 | 4.59E-02 | -0.98 | 1.77E-03 |
| TEAD2 | 0.61 | 3.67E-02 | 0.89 | 1.13E-04 | -1.05 | 6.13E-05 |
| TFPI | 0.43 | 5.87E-04 | 0.68 | 1.53E-06 | -0.59 | 7.34E-03 |
| TFRC | 0.75 | 2.07E-10 | 1.35 | 1.45E-11 | -1.05 | 4.80E-09 |
| THSD1 | 0.49 | 6.04E-02 | 1.47 | 1.19E-02 | -1.08 | 2.17E-03 |
| TK1 | 0.48 | 5.08E-02 | 0.70 | 4.80E-03 | -1.62 | 3.08E-05 |
| TM6SF1 | 1.89 | 8.97E-03 | 2.41 | 2.93E-03 | -2.01 | 3.73E-03 |
| TMBIM1 | 0.27 | 1.88E-02 | 0.41 | 4.36E-07 | -0.64 | 1.68E-04 |

| | | | | | | |
|---|---|---|---|---|---|---|
| TMEM130 | 1.57 | 5.83E-03 | 1.48 | 6.37E-02 | -1.93 | 4.88E-02 |
| TMEM131L | 0.42 | 6.31E-02 | 0.65 | 1.48E-03 | -1.08 | 4.53E-03 |
| TMEM171 | 1.13 | 7.32E-02 | 1.46 | 3.69E-04 | -2.07 | 1.84E-05 |
| TMEM2 | 0.40 | 8.64E-02 | 0.44 | 3.13E-04 | -0.77 | 4.30E-05 |
| TMEM265 | 0.39 | 1.30E-03 | 0.33 | 6.30E-02 | -0.43 | 3.18E-04 |
| TMEM40 | 0.40 | 8.90E-02 | 0.51 | 2.73E-03 | -0.53 | 1.32E-03 |
| TMEM51 | 0.50 | 7.75E-10 | 0.56 | 1.17E-05 | -0.82 | 1.06E-03 |
| TMEM64 | 0.36 | 2.51E-03 | 0.39 | 6.22E-04 | -0.32 | 5.20E-05 |
| TMPRSS2 | 0.57 | 3.14E-03 | 0.83 | 1.51E-11 | -0.56 | 2.48E-02 |
| TMSB10P1 | 0.74 | 6.16E-03 | 0.71 | 3.10E-02 | -0.52 | 4.42E-04 |
| TMSB4X | 0.38 | 1.69E-02 | 0.49 | 5.25E-06 | -0.81 | 8.06E-04 |
| TMSB4XP6 | 0.77 | 1.21E-03 | 0.65 | 9.47E-03 | -0.71 | 1.54E-02 |
| TNF | 1.22 | 3.58E-03 | 1.32 | 3.07E-02 | -2.09 | 2.58E-03 |
| TNFAIP3 | 0.63 | 1.89E-02 | 0.63 | 5.91E-06 | -0.88 | 1.95E-02 |
| TNFRSF10B | 0.29 | 1.05E-02 | 0.36 | 2.72E-04 | -0.63 | 3.50E-03 |
| TNFRSF13C | 1.60 | 9.78E-02 | 1.66 | 9.27E-02 | -2.22 | 9.73E-06 |
| TNFRSF6B | 0.95 | 1.13E-03 | 0.79 | 2.54E-04 | -0.92 | 4.39E-02 |
| TNNT1 | 1.00 | 2.52E-03 | 0.75 | 1.44E-02 | -0.97 | 2.17E-04 |
| TNPO2 | 0.18 | 2.26E-02 | 0.22 | 3.78E-02 | -0.37 | 1.36E-02 |
| TP53BP2 | 0.31 | 7.56E-04 | 0.25 | 2.78E-02 | -0.17 | 2.29E-02 |
| TPM3 | 0.19 | 6.49E-02 | 0.27 | 3.41E-04 | -0.48 | 1.85E-02 |
| TRAF3IP2 | 0.19 | 3.77E-02 | 0.27 | 2.18E-02 | -0.50 | 1.83E-02 |
| TRIM14 | 0.53 | 4.64E-09 | 0.49 | 4.87E-06 | -0.35 | 1.62E-03 |
| TRIM61 | 1.15 | 7.44E-03 | 1.63 | 2.15E-04 | -1.40 | 3.70E-04 |
| TRIT1 | 0.56 | 5.72E-05 | 0.52 | 2.40E-04 | -0.35 | 3.58E-02 |
| TRPC6 | 3.50 | 1.63E-03 | 3.51 | 6.42E-36 | -3.28 | 4.99E-06 |
| TSPAN5 | 0.66 | 8.30E-09 | 0.60 | 9.45E-05 | -0.30 | 2.93E-02 |
| TTC28 | 1.43 | 1.83E-02 | 1.75 | 2.84E-04 | -1.28 | 2.63E-04 |
| TXK | 2.25 | 9.99E-03 | 2.50 | 3.13E-03 | -2.63 | 8.86E-03 |
| UAP1L1 | 0.79 | 8.09E-04 | 0.71 | 6.75E-03 | -1.16 | 9.51E-07 |
| UBALD2 | 0.27 | 1.31E-02 | 0.33 | 5.54E-03 | -0.40 | 9.86E-05 |
| UBASH3B | 0.28 | 2.56E-02 | 0.45 | 5.65E-04 | -1.06 | 2.79E-03 |
| UGDH | 0.42 | 1.94E-03 | 0.51 | 4.91E-06 | -0.33 | 7.28E-03 |
| UGT1A1 | 0.49 | 4.08E-03 | 0.66 | 2.60E-08 | -0.55 | 8.90E-03 |
| UGT1A10 | 0.49 | 3.71E-03 | 0.66 | 3.51E-08 | -0.56 | 7.66E-03 |
| UGT1A3 | 0.49 | 4.03E-03 | 0.65 | 2.21E-08 | -0.54 | 9.22E-03 |
| UGT1A4 | 0.49 | 3.89E-03 | 0.66 | 1.93E-08 | -0.55 | 8.65E-03 |
| UGT1A5 | 0.49 | 3.99E-03 | 0.65 | 2.43E-08 | -0.54 | 9.27E-03 |
| UGT1A6 | 0.48 | 3.98E-03 | 0.67 | 1.93E-09 | -0.56 | 7.03E-03 |
| UGT1A7 | 0.49 | 3.05E-03 | 0.65 | 1.38E-08 | -0.54 | 9.16E-03 |
| UGT1A8 | 0.49 | 3.79E-03 | 0.65 | 2.43E-08 | -0.54 | 9.23E-03 |
| UGT1A9 | 0.49 | 3.90E-03 | 0.65 | 2.23E-08 | -0.54 | 9.21E-03 |
| UHRF1 | 0.64 | 6.79E-02 | 0.84 | 7.05E-05 | -1.44 | 1.05E-03 |
| ULBP1 | 1.32 | 1.28E-02 | 1.97 | 5.10E-04 | -1.59 | 3.55E-02 |
| UNC13D | 1.17 | 1.72E-03 | 2.67 | 3.46E-26 | -3.15 | 5.17E-09 |
| UPP1 | 0.32 | 1.94E-03 | 0.44 | 3.11E-04 | -0.57 | 3.55E-03 |
| USP10 | 0.21 | 7.81E-02 | 0.25 | 1.71E-02 | -0.13 | 2.77E-02 |
| USP32 | 0.20 | 5.08E-02 | 0.19 | 8.04E-02 | -0.22 | 2.00E-04 |
| USP44 | 1.58 | 1.72E-02 | 2.47 | 2.50E-06 | -1.44 | 8.38E-03 |

| | | | | | | |
|---|---|---|---|---|---|---|
| VAMP5 | 0.79 | 7.56E-05 | 0.86 | 3.62E-05 | -0.49 | 8.29E-03 |
| VAT1 | 0.37 | 4.72E-02 | 0.68 | 4.86E-07 | -0.98 | 1.01E-03 |
| VAV2 | 0.44 | 5.50E-05 | 0.62 | 4.08E-10 | -0.65 | 1.06E-04 |
| VCAM1 | 2.15 | 2.19E-03 | 2.15 | 1.38E-03 | -2.69 | 3.01E-02 |
| VCL | 0.57 | 4.40E-21 | 0.62 | 4.04E-10 | -0.69 | 1.27E-03 |
| VDAC1 | 0.29 | 4.95E-05 | 0.23 | 2.73E-02 | -0.26 | 1.08E-03 |
| VEGFA | 0.67 | 1.60E-02 | 0.52 | 1.14E-05 | -0.42 | 1.09E-02 |
| VEGFC | 0.50 | 1.05E-02 | 0.69 | 1.97E-03 | -0.80 | 3.94E-04 |
| VNN2 | 2.31 | 4.12E-02 | 1.37 | 5.31E-06 | -1.69 | 4.15E-06 |
| WDR1 | 0.23 | 5.77E-05 | 0.35 | 9.94E-07 | -0.26 | 3.79E-02 |
| WDR18 | 0.26 | 1.26E-02 | 0.36 | 5.97E-04 | -0.29 | 1.07E-04 |
| WNT5A | 1.08 | 3.19E-08 | 1.97 | 2.46E-20 | -0.80 | 1.06E-04 |
| WNT7A | 0.36 | 8.02E-02 | 1.34 | 1.09E-24 | -1.47 | 1.01E-04 |
| WTIP | 0.22 | 9.31E-02 | 0.29 | 6.74E-02 | -0.46 | 9.21E-07 |
| WWC2 | 0.30 | 5.53E-04 | 0.27 | 4.36E-02 | -0.30 | 3.15E-02 |
| XDH | 0.57 | 3.20E-02 | 2.55 | 1.68E-03 | -1.25 | 1.00E-02 |
| XXYLT1 | 0.35 | 6.04E-04 | 0.48 | 1.69E-04 | -0.49 | 2.08E-07 |
| ZFAS1 | 0.35 | 7.80E-04 | 0.48 | 2.60E-05 | -0.58 | 6.92E-08 |
| ZFP92 | 1.08 | 9.44E-02 | 1.53 | 5.78E-02 | -2.22 | 7.63E-04 |
| ZIK1 | 0.29 | 9.97E-02 | 0.39 | 5.41E-02 | -0.50 | 5.12E-03 |
| ZNF134 | 0.21 | 4.44E-02 | 0.21 | 8.08E-02 | -0.28 | 1.28E-03 |
| ZNF154 | 0.98 | 2.60E-05 | 1.05 | 7.54E-05 | -0.87 | 9.63E-05 |
| ZNF257 | 2.89 | 7.33E-03 | 3.35 | 3.53E-03 | -3.33 | 2.57E-04 |
| ZNF266 | 0.56 | 9.90E-04 | 0.61 | 3.17E-07 | -0.53 | 2.75E-02 |
| ZNF320 | 0.36 | 4.39E-02 | 0.64 | 1.15E-04 | -0.54 | 2.91E-03 |
| ZNF429 | 1.03 | 4.77E-15 | 1.13 | 1.19E-14 | -0.50 | 4.12E-02 |
| ZNF528 | 0.76 | 9.31E-08 | 0.96 | 7.84E-13 | -0.59 | 5.69E-04 |
| ZNF618 | 0.54 | 8.43E-05 | 0.64 | 3.06E-06 | -1.21 | 8.03E-06 |
| ZNF626 | 0.70 | 5.37E-05 | 0.92 | 1.20E-09 | -0.43 | 2.28E-03 |
| ZNF677 | 0.46 | 4.92E-02 | 0.54 | 5.29E-02 | -0.78 | 5.58E-03 |
| ZNF702P | 0.40 | 1.75E-02 | 0.49 | 6.81E-03 | -0.68 | 1.90E-05 |
| ZNF710 | 0.19 | 3.21E-02 | 0.28 | 3.12E-02 | -0.38 | 4.44E-12 |
| ZNF826P | 0.96 | 3.57E-02 | 1.31 | 1.43E-04 | -0.59 | 6.84E-03 |
| ZP3 | 0.63 | 9.68E-02 | 1.36 | 9.31E-04 | -1.58 | 1.56E-05 |

**Table S3. IL-6-related genes upregulated in distal and honeycomb cultures.** Genes upregulated in distal and honeycomb cultures from Table S2 which are also upregulated in airway epithelial cultures after treatment with IL-6 (GSE 113185). Log2 fold change (L2FC) and *P*-value shown.

| **Gene** | **Proximal (up day 14 vs day 0)** | | **Distal (down day 14 vs proximal day 14)** | | **Honeycomb (down day 14 vs proximal day 14)** | |
|---|---|---|---|---|---|---|
| | L2FC | *P*-value | L2FC | *P*-value | L2FC | *P*-value |
| ADA | -1.285 | 2.45E-04 | 0.830 | 7.03E-04 | 0.980 | 3.75E-08 |
| ADRB2 | -0.540 | 2.35E-07 | 0.494 | 2.15E-04 | 0.980 | 3.82E-11 |
| ALDH1A2 | -1.313 | 6.18E-04 | 2.141 | 3.01E-06 | 3.082 | 3.77E-12 |
| ANXA3 | -1.582 | 3.52E-05 | 0.712 | 2.59E-12 | 1.287 | 1.25E-28 |
| ANXA8 | -0.721 | 1.22E-03 | 0.502 | 1.10E-02 | 0.594 | 3.33E-07 |
| APOBEC3G | -0.637 | 4.81E-05 | 0.661 | 1.17E-04 | 0.517 | 1.11E-03 |
| APOE | -2.382 | 1.06E-15 | 1.185 | 3.05E-06 | 1.697 | 4.93E-14 |
| ARL16 | -0.390 | 1.88E-04 | 0.458 | 2.01E-06 | 0.454 | 1.71E-04 |
| ARL6IP5 | -0.536 | 1.54E-05 | 0.424 | 1.34E-12 | 0.528 | 2.00E-14 |
| ARNTL2 | -0.445 | 1.55E-05 | 0.243 | 6.81E-04 | 0.375 | 4.40E-04 |
| ARPC5L | -0.202 | 4.13E-03 | 0.260 | 1.24E-05 | 0.360 | 2.15E-04 |
| ASL | -0.322 | 5.96E-03 | 0.185 | 1.55E-02 | 0.394 | 4.95E-05 |
| ATG10 | -0.739 | 1.56E-04 | 0.768 | 3.62E-05 | 0.907 | 1.61E-05 |
| ATP13A4 | -1.183 | 9.22E-12 | 0.951 | 6.49E-07 | 1.739 | 5.13E-31 |
| ATP6V1B2 | -0.401 | 7.95E-08 | 0.302 | 9.69E-06 | 0.365 | 4.79E-05 |
| BAK1 | -0.494 | 4.02E-18 | 0.311 | 1.62E-02 | 0.357 | 7.85E-04 |
| BCL2A1 | -2.691 | 2.02E-07 | 1.762 | 1.26E-07 | 2.813 | 5.93E-16 |
| BMP2 | -0.774 | 1.68E-03 | 0.381 | 1.31E-03 | 0.409 | 7.21E-03 |
| BPHL | -0.358 | 2.28E-04 | 0.395 | 7.43E-04 | 0.465 | 3.80E-04 |
| BTN3A2 | -1.453 | 9.30E-03 | 2.437 | 4.11E-71 | 2.445 | 5.50E-108 |
| BZW2 | -0.307 | 2.02E-04 | 0.349 | 7.41E-06 | 0.255 | 5.83E-03 |
| C15orf48 | -1.482 | 4.99E-05 | 0.837 | 1.15E-13 | 1.563 | 1.84E-06 |
| C19orf48 | -0.394 | 3.08E-06 | 0.408 | 1.74E-07 | 0.440 | 2.46E-06 |
| CAP1 | -0.410 | 3.49E-03 | 0.217 | 2.72E-03 | 0.355 | 4.51E-07 |
| CAPG | -0.637 | 6.39E-10 | 0.381 | 9.08E-05 | 0.366 | 2.58E-03 |
| CAPN12 | -1.468 | 6.41E-09 | 1.265 | 1.62E-03 | 1.092 | 1.00E-06 |
| CAPN14 | -1.330 | 5.38E-03 | 0.932 | 3.12E-04 | 1.863 | 4.75E-03 |
| CARD19 | -0.451 | 5.47E-06 | 0.330 | 6.14E-06 | 0.264 | 6.67E-03 |
| CASP10 | -0.406 | 1.50E-08 | 0.272 | 1.08E-03 | 0.385 | 6.96E-03 |
| CBS | -1.181 | 9.90E-04 | 1.226 | 3.54E-07 | 1.565 | 4.20E-07 |
| CCL2 | -2.912 | 3.16E-03 | 5.384 | 9.72E-07 | 5.915 | 1.68E-08 |

| | | | | | | |
|---|---|---|---|---|---|---|
| CD274 | -0.797 | 5.55E-03 | 0.538 | 8.62E-03 | 0.829 | 1.59E-07 |
| CD40 | -0.705 | 1.85E-07 | 0.878 | 2.62E-05 | 1.004 | 5.40E-12 |
| CD46 | -0.216 | 2.00E-03 | 0.387 | 8.07E-04 | 0.428 | 6.09E-08 |
| CHI3L2 | -3.095 | 5.69E-06 | 2.565 | 5.87E-04 | 4.451 | 1.51E-08 |
| CIB2 | -1.810 | 4.20E-32 | 1.058 | 3.59E-04 | 1.349 | 2.66E-05 |
| CKAP2 | -0.831 | 1.94E-24 | 0.238 | 1.07E-02 | 0.489 | 1.55E-03 |
| CSTB | -0.771 | 5.74E-03 | 0.714 | 2.36E-03 | 0.804 | 5.96E-09 |
| CTSE | -3.032 | 9.50E-07 | 3.763 | 2.91E-19 | 5.970 | 1.29E-120 |
| DCTN5 | -0.463 | 1.65E-14 | 0.611 | 5.62E-19 | 0.597 | 1.32E-11 |
| DEFB4A | -4.644 | 7.90E-09 | 2.782 | 1.09E-06 | 6.942 | 8.31E-09 |
| DST | -0.961 | 3.24E-09 | 0.284 | 1.51E-02 | 0.421 | 3.03E-06 |
| EBI3 | -2.466 | 5.00E-05 | 1.864 | 1.79E-04 | 2.878 | 5.53E-09 |
| ECI2 | -0.583 | 4.67E-06 | 0.536 | 1.20E-08 | 0.535 | 5.82E-05 |
| EDA | -0.624 | 2.74E-04 | 1.298 | 1.54E-04 | 1.491 | 6.98E-13 |
| EDN1 | -2.204 | 5.55E-04 | 0.832 | 4.98E-04 | 1.611 | 1.65E-09 |
| EIF2S2 | -0.191 | 3.07E-03 | 0.173 | 3.73E-03 | 0.349 | 2.11E-05 |
| EIF6 | -0.349 | 6.51E-08 | 0.238 | 3.56E-03 | 0.326 | 2.51E-05 |
| ELOVL6 | -0.816 | 7.94E-05 | 0.547 | 1.80E-06 | 0.598 | 2.46E-09 |
| EMP1 | -2.096 | 1.88E-06 | 0.394 | 4.13E-03 | 0.683 | 2.03E-13 |
| ENO1 | -0.235 | 8.83E-03 | 0.338 | 3.48E-04 | 0.369 | 2.89E-07 |
| EPSTI1 | -2.035 | 5.72E-10 | 1.010 | 4.97E-05 | 1.255 | 1.02E-07 |
| FAH | -0.332 | 6.85E-03 | 0.280 | 1.76E-03 | 0.317 | 2.74E-03 |
| FAM89A | -1.150 | 1.62E-05 | 0.928 | 1.78E-04 | 0.952 | 2.32E-04 |
| FLRT3 | -0.289 | 4.48E-03 | 0.545 | 3.08E-09 | 0.837 | 1.26E-18 |
| GALNT14 | -0.879 | 3.90E-03 | 0.623 | 1.50E-07 | 1.033 | 2.27E-10 |
| GARS | -0.360 | 7.33E-03 | 0.403 | 4.40E-07 | 0.709 | 1.80E-07 |
| GBP1 | -1.037 | 2.62E-03 | 0.709 | 1.26E-12 | 0.818 | 8.17E-11 |
| GBP2 | -0.296 | 6.12E-04 | 0.615 | 6.98E-09 | 0.434 | 1.73E-04 |
| GCNT2 | -0.209 | 2.85E-03 | 0.295 | 9.03E-03 | 0.237 | 2.85E-03 |
| GGH | -0.812 | 6.26E-13 | 0.479 | 1.82E-09 | 0.304 | 1.45E-02 |
| GNG5 | -0.189 | 8.48E-03 | 0.222 | 5.74E-03 | 0.253 | 9.72E-04 |
| GPCPD1 | -0.497 | 2.55E-03 | 0.352 | 1.55E-03 | 0.872 | 4.51E-06 |
| GPR108 | -0.221 | 1.27E-02 | 0.201 | 1.63E-02 | 0.276 | 1.20E-03 |
| GSTM3 | -1.910 | 1.58E-11 | 1.813 | 1.32E-05 | 2.400 | 1.24E-11 |
| HDHD3 | -0.686 | 6.77E-03 | 0.483 | 1.48E-04 | 0.701 | 2.11E-05 |
| HOPX | -1.677 | 8.36E-03 | 1.458 | 1.96E-10 | 2.752 | 6.78E-50 |
| HSD17B1 | -0.682 | 2.90E-04 | 0.667 | 5.77E-04 | 0.666 | 6.70E-03 |
| IDO1 | -1.860 | 1.36E-04 | 1.122 | 1.00E-02 | 1.556 | 7.33E-13 |
| IFI27 | -3.981 | 7.32E-26 | 1.586 | 1.55E-03 | 2.743 | 1.34E-28 |

| | | | | | | |
|---|---|---|---|---|---|---|
| IFI27L2 | -0.849 | 3.40E-07 | 0.499 | 1.67E-03 | 0.457 | 1.26E-03 |
| IFI6 | -2.164 | 8.96E-14 | 0.865 | 2.13E-05 | 1.376 | 1.11E-16 |
| IFIT1 | -2.639 | 1.44E-07 | 1.334 | 1.18E-02 | 0.879 | 3.66E-03 |
| IFIT2 | -1.020 | 7.44E-03 | 0.783 | 5.24E-19 | 0.486 | 1.37E-04 |
| IFIT3 | -1.450 | 3.08E-05 | 0.853 | 4.43E-08 | 0.791 | 5.65E-09 |
| IL1A | -2.154 | 3.18E-04 | 0.636 | 1.30E-04 | 2.148 | 4.42E-07 |
| IL1B | -3.550 | 8.69E-05 | 0.667 | 5.43E-03 | 2.362 | 4.09E-04 |
| IRF9 | -0.689 | 5.21E-19 | 0.408 | 1.20E-07 | 0.407 | 7.32E-06 |
| KCNJ15 | -0.571 | 2.56E-05 | 0.448 | 2.37E-03 | 0.650 | 5.56E-10 |
| KLHL5 | -0.424 | 5.36E-03 | 0.210 | 1.26E-02 | 0.250 | 4.22E-03 |
| KRT8 | -0.513 | 6.44E-10 | 0.222 | 9.54E-03 | 0.234 | 2.22E-03 |
| LCP1 | -2.906 | 1.40E-07 | 1.904 | 6.52E-14 | 2.605 | 3.02E-16 |
| LDHB | -0.362 | 1.84E-04 | 0.271 | 1.12E-03 | 0.163 | 1.68E-02 |
| LEMD1 | -1.760 | 7.07E-05 | 1.127 | 4.76E-03 | 1.407 | 5.00E-03 |
| LINC00960 | -1.670 | 9.09E-05 | 1.803 | 1.68E-02 | 2.028 | 1.34E-03 |
| LY6K | -1.255 | 6.86E-03 | 1.202 | 4.13E-04 | 1.520 | 4.82E-05 |
| MAPK3 | -0.344 | 1.56E-03 | 0.378 | 2.40E-05 | 0.455 | 6.08E-07 |
| MELTF | -1.505 | 7.76E-06 | 1.221 | 6.88E-05 | 1.824 | 8.54E-28 |
| MFSD3 | -0.307 | 1.10E-02 | 0.465 | 4.49E-08 | 0.571 | 1.08E-08 |
| MILR1 | -1.722 | 5.61E-06 | 1.949 | 2.58E-05 | 2.164 | 1.24E-15 |
| MMD | -0.699 | 1.39E-03 | 0.578 | 8.28E-08 | 0.842 | 9.50E-11 |
| MMP1 | -1.349 | 8.02E-06 | 1.671 | 5.86E-14 | 3.431 | 1.02E-06 |
| MSRB2 | -0.185 | 3.12E-03 | 0.244 | 2.03E-03 | 0.403 | 5.60E-05 |
| NCAM2 | -2.376 | 6.20E-03 | 2.336 | 9.34E-04 | 3.717 | 2.59E-06 |
| NDC1 | -0.479 | 7.38E-06 | 0.245 | 4.26E-03 | 0.250 | 1.97E-02 |
| NIPSNAP1 | -0.389 | 3.83E-06 | 0.283 | 4.53E-04 | 0.352 | 4.77E-05 |
| NMD3 | -0.217 | 4.87E-04 | 0.272 | 1.65E-04 | 0.304 | 3.40E-04 |
| NME4 | -0.404 | 3.05E-03 | 0.350 | 1.93E-03 | 0.503 | 1.94E-06 |
| NRIP1 | -0.784 | 3.92E-04 | 0.497 | 2.07E-05 | 0.574 | 5.51E-09 |
| NT5E | -2.112 | 1.90E-06 | 0.734 | 4.07E-04 | 1.905 | 9.70E-57 |
| NUDT2 | -0.573 | 2.46E-06 | 0.505 | 3.93E-03 | 0.632 | 1.84E-05 |
| OAS1 | -0.647 | 1.00E-02 | 0.344 | 4.71E-05 | 0.335 | 1.96E-02 |
| OASL | -1.186 | 2.48E-03 | 1.695 | 4.27E-16 | 1.036 | 4.82E-03 |
| OPA1 | -0.226 | 5.42E-04 | 0.280 | 5.56E-05 | 0.332 | 7.08E-05 |
| OSGIN2 | -0.238 | 1.01E-03 | 0.290 | 1.97E-03 | 0.427 | 8.34E-05 |
| PAK1 | -0.359 | 7.72E-04 | 0.387 | 2.34E-07 | 0.540 | 1.60E-11 |
| PARP9 | -0.357 | 1.31E-03 | 0.317 | 3.21E-03 | 0.453 | 4.87E-05 |
| PDCD5 | -0.360 | 4.21E-03 | 0.398 | 3.94E-07 | 0.455 | 1.60E-07 |
| PDE4C | -2.561 | 5.51E-05 | 2.129 | 2.79E-07 | 2.010 | 1.70E-05 |

| | | | | | | |
|---|---|---|---|---|---|---|
| PLIN2 | -0.451 | 1.14E-03 | 0.603 | 1.23E-04 | 0.494 | 1.14E-07 |
| POP1 | -1.019 | 1.64E-09 | 0.580 | 4.15E-06 | 0.795 | 4.01E-04 |
| PPA1 | -0.154 | 1.93E-03 | 0.335 | 6.08E-04 | 0.451 | 2.08E-07 |
| PRELID1 | -0.266 | 2.79E-03 | 0.225 | 3.11E-04 | 0.256 | 2.73E-03 |
| PRSS22 | -0.329 | 5.52E-04 | 0.556 | 5.96E-16 | 0.739 | 7.84E-06 |
| PSCA | -2.744 | 9.09E-03 | 2.192 | 1.63E-04 | 2.724 | 1.04E-03 |
| RAB32 | -0.770 | 1.00E-04 | 0.389 | 2.79E-05 | 0.669 | 5.22E-10 |
| RASGEF1A | -1.957 | 3.60E-05 | 1.174 | 1.55E-05 | 1.479 | 1.98E-05 |
| RCAN1 | -0.583 | 5.09E-03 | 0.236 | 1.04E-02 | 0.643 | 8.14E-11 |
| RGS10 | -1.382 | 5.65E-06 | 0.421 | 1.66E-03 | 0.451 | 8.84E-03 |
| RGS20 | -1.842 | 2.00E-07 | 0.705 | 3.74E-05 | 0.803 | 1.74E-04 |
| RHOF | -2.126 | 7.52E-25 | 1.663 | 4.01E-51 | 2.186 | 1.30E-75 |
| RND3 | -0.633 | 6.71E-03 | 0.277 | 2.26E-03 | 0.332 | 5.74E-06 |
| RNF216P1 | -0.396 | 2.41E-05 | 0.516 | 3.55E-06 | 0.676 | 1.78E-06 |
| RPL29 | -0.374 | 2.28E-05 | 0.263 | 1.66E-02 | 0.258 | 2.96E-04 |
| RRP7A | -0.246 | 1.07E-04 | 0.297 | 1.55E-04 | 0.352 | 8.79E-06 |
| SARS | -0.257 | 1.75E-03 | 0.266 | 1.80E-04 | 0.330 | 4.40E-04 |
| SAT1 | -0.179 | 1.59E-05 | 0.190 | 4.62E-04 | 0.295 | 3.24E-04 |
| SCRN2 | -0.462 | 7.09E-11 | 0.289 | 1.93E-03 | 0.507 | 9.03E-06 |
| SERPINB7 | -0.906 | 2.43E-04 | 0.567 | 4.22E-04 | 2.376 | 2.36E-04 |
| SFN | -0.909 | 5.09E-06 | 0.315 | 4.36E-03 | 0.588 | 1.56E-07 |
| SLC16A1 | -0.536 | 1.00E-03 | 0.709 | 1.05E-07 | 0.733 | 1.94E-06 |
| SNCG | -2.414 | 4.90E-15 | 0.856 | 9.87E-04 | 0.807 | 5.16E-03 |
| SNHG5 | -1.768 | 1.43E-04 | 1.949 | 4.10E-14 | 1.947 | 1.60E-26 |
| SNHG8 | -0.323 | 1.03E-03 | 0.418 | 4.25E-03 | 0.313 | 2.02E-03 |
| SNRPF | -0.307 | 3.50E-04 | 0.228 | 1.09E-02 | 0.264 | 4.55E-03 |
| SPRR2A | -4.754 | 4.21E-22 | 1.384 | 4.55E-05 | 5.193 | 3.87E-05 |
| SPRR2D | -4.083 | 1.22E-16 | 1.486 | 9.10E-07 | 3.924 | 4.52E-05 |
| SRPX2 | -1.082 | 3.77E-10 | 0.935 | 5.55E-13 | 0.942 | 5.83E-15 |
| STC2 | -1.612 | 1.17E-03 | 1.459 | 8.28E-07 | 2.145 | 3.20E-06 |
| STRIP2 | -1.023 | 3.50E-04 | 1.217 | 4.88E-04 | 1.405 | 2.97E-07 |
| TAP1 | -0.607 | 5.24E-07 | 0.388 | 3.22E-06 | 0.495 | 3.14E-10 |
| TEAD2 | -1.047 | 3.64E-06 | 0.608 | 4.08E-03 | 0.890 | 7.48E-06 |
| TFRC | -1.046 | 8.91E-11 | 0.753 | 1.21E-12 | 1.352 | 2.29E-13 |
| TMEM265 | -0.427 | 2.44E-05 | 0.387 | 5.60E-05 | 0.326 | 1.20E-02 |
| TMEM40 | -0.527 | 1.35E-04 | 0.398 | 1.43E-02 | 0.505 | 2.79E-04 |
| TMEM51 | -0.823 | 1.03E-04 | 0.502 | 5.40E-12 | 0.564 | 6.04E-07 |
| TMSB4X | -0.808 | 7.36E-05 | 0.377 | 1.44E-03 | 0.490 | 2.49E-07 |
| TNF | -2.090 | 3.04E-04 | 1.219 | 1.96E-04 | 1.320 | 4.84E-03 |

| | | | | | | |
|---|---|---|---|---|---|---|
| TNFRSF6B | -0.918 | 1.09E-02 | 0.952 | 4.72E-05 | 0.794 | 1.85E-05 |
| TNNT1 | -0.971 | 1.56E-05 | 1.004 | 1.24E-04 | 0.751 | 1.99E-03 |
| TPM3 | -0.484 | 3.56E-03 | 0.185 | 8.98E-03 | 0.272 | 2.59E-05 |
| TRIT1 | -0.352 | 8.36E-03 | 0.560 | 1.40E-06 | 0.523 | 1.73E-05 |
| TSPAN5 | -0.305 | 6.40E-03 | 0.663 | 7.04E-11 | 0.595 | 6.09E-06 |
| UGT1A6 | -0.559 | 1.04E-03 | 0.482 | 2.26E-04 | 0.669 | 4.30E-11 |
| UPP1 | -0.566 | 4.48E-04 | 0.324 | 9.02E-05 | 0.443 | 2.33E-05 |
| VAMP5 | -0.492 | 1.29E-03 | 0.785 | 1.95E-06 | 0.858 | 2.12E-06 |
| VDAC1 | -0.256 | 1.05E-04 | 0.287 | 1.18E-06 | 0.233 | 4.22E-03 |
| VNN2 | -1.693 | 1.67E-07 | 2.312 | 4.77E-03 | 1.365 | 2.53E-07 |
| ZFAS1 | -0.577 | 1.75E-09 | 0.352 | 3.02E-05 | 0.479 | 1.45E-06 |
| ZNF320 | -0.539 | 3.52E-04 | 0.361 | 5.20E-03 | 0.641 | 7.67E-06 |
| ZNF429 | -0.502 | 1.00E-02 | 1.032 | 1.53E-17 | 1.126 | 1.16E-16 |
| ZNF626 | -0.433 | 2.63E-04 | 0.704 | 1.30E-06 | 0.923 | 2.55E-11 |
| ZNF702P | -0.677 | 9.36E-07 | 0.399 | 1.50E-03 | 0.485 | 8.13E-04 |
| ZP3 | -1.576 | 7.50E-07 | 0.626 | 1.61E-02 | 1.360 | 8.08E-05 |

**Table S4. Primers used for gene expression assay**

| Gene | Product ID |
|---|---|
| *KRT5* | Hs00361185_m1 |
| *KRT6A* | Hs01699781_g1 |
| *KRT8* | Hs01595539_g1 |
| *KRT14* | Hs00265033_m1 |
| *KRT17* | Hs01555135_g1 |
| *IL1B* | Hs01555410_m1 |
| *IL6* | Hs00174131_m1 |
| *IL11* | Hs01055414_m1 |
| *IL6R* | Hs01075664_m1 |
| *IL6ST* | Hs00174360_m1 |
| *EGFR* | Hs0176090_m1 |
| *ERBB2* | Hs01001580_m1 |
| *EGF* | Hs01099990_m1 |
| *AREG* | Hs00950669_m1 |
| *CTGF* | Hs00170014_m1 |
| *CYR61* | Hs00155479_m1 |
| *CD44* | Hs01075864_m1 |
| *TNF* | Hs00174128_m1 |
| *LAMA5* | Hs00966585_m1 |
| *LAMB1* | Hs01055960_m1 |
| *LAMC1* | Hs00267056_m1 |
| *COL1A1* | Hs00164004_m1 |
| *ITGB1* | Hs05351551_g1 |
| *ITGB4* | Hs00236216_m1 |
| *ITGA6* | Hs01041011_m1 |
| *MUC5B* | Hs00861595_m1 |
| *FOXJ1* | Hs00230964_m1 |
| *CDH1* | Hs01023895_m1 |
| *SNAI1* | Hs00195591_m1 |
| *ZEB1* | Hs00232783_m1 |
| *ACTB* | Hs01060665_g1 |

**Movie S1.** Precision cut lung slice (PCLS) of uninjured airway in Krt5-CreERT2/tdTomato mouse. Non-migratory airways labeled with EpCAM can be observed without presence of $Krt5^+$ cells. Images were acquired every 10 minutes for 18 hours at 20x magnification.

**Movie S2.** Precision cut lung slice (PCLS) of H1N1-injured airway in Krt5-CreERT2/tdTomato mouse harvested on day 11 after injury. Fluidized airways labeled with EpCAM can be observed with the presence of $Krt5^+$ cells. Images were acquired every 8 minutes for 18 hours at 20x magnification.

**Movie S3.** Precision cut lung slice (PCLS) of bleomycin-injured airway in Krt5-CreERT2/tdTomato mouse harvested on day 21 after injury. Fluidized airways labeled with EpCAM can be observed with the presence of $Krt5^+$ cells. Images were acquired every 8 minutes for 18 hours at 20x magnification.

**Movie S4.** Proximal cultures untreated and stimulated with IL-6 and sIL-6R on day 14 of air-liquid interface (ALI). Epithelia transition into a fluidized phase after treatment. Images were acquired every 20 minutes for 48 hours at 10x magnification.

**Movie S5.** Distal cultures untreated and inhibited with anti-IL-6R antibody on day 14 of air-liquid interface (ALI). Epithelia transition from a fluidized to solid-like phase after treatment. Images were acquired every 20 minutes for 48 hours at 10x magnification.

**Movie S6.** Honeycomb cultures untreated and inhibited with anti-IL-6R antibody on day 14 of air-liquid interface (ALI). Epithelia transition from a fluidized to solid-like phase after treatment. Images were acquired every 20 minutes for 48 hours at 10x magnification.

**Movie S7.** Treatment of H1N1-injured precision cut lung slice (PCLS) with blebbistatin prevents fluidization of airway epithelia. Images were acquired every 8 minutes for 18 hours at 20x magnification.

**Movie S8.** Treatment of H1N1-injured precision cut lung slice (PCLS) with anti-IL-6 and anti-IL-6R antibodies prevents fluidization of airway epithelia. Images were acquired every 8 minutes for 18 hours at 20x magnification.

**Movie S9.** Treatment of H1N1-injured precision cut lung slice (PCLS) with ruxolitinib (JAK1/2 inhibitor) does not prevent fluidization of airway epithelia. Images were acquired every 8 minutes for 18 hours at 20x magnification.

**Movie S10.** Treatment of H1N1-injured precision cut lung slice (PCLS) with saracatinib (SFK inhibitor) prevents fluidization of airway epithelia. Images were acquired every 8 minutes for 18 hours at 20x magnification.

**Data file S1**. Raw data for all experiments where $n<20$.